Government of Saskatchewan
Ministry of Agriculture

ADF Project Progress Report Format

1. Project title, ADF file number and reporting period.

Title	**Oat Lodging: Identifying key root and shoot traits for improved standability**
File Number	ADF20210755; WGRF: VarD2227
Scientific Reporting Period	April 1st 2022 – June 1st 2023
Financial Reporting Period	April 1st 2022 – March 31st 2023

2. Name of the Principal Investigator and contact information.

Principal Investigator (PI)	**Allan Feurtado**, Associate Research Officer
Address	Aquatic and Crop Resource Development National Research Council Canada / Government of Canada 110 Gymnasium Place, Saskatoon, SK S7N 0W9
Phone	Mobile: 306-491-0127
Email	Allan.Feurtado@nrc-cnrc.gc.ca

3. Name of the collaborators and contact information

Co-PI	**Aaron Beattie**, Associate Professor, Barley and Oat Breeding Program
Address	Crop Development Centre, University of Saskatchewan Agriculture Building, 51 Campus Dr., Saskatoon, SK, S7N 5A8
Phone	Office: 306-966-2102
Email	Aaron.Beattie@usask.ca

Collaborator	**Scott Noble**, Associate Professor
Address	Department of Mechanical Engineering, University of Saskatchewan Agriculture Building, 57 Campus Dr., Saskatoon, SK, S7N 5A9
Phone	Office: 306-966-5308
Email	Noble, Scott <sdn179@mail.usask.ca>

Collaborator	**Leon Kochian**, Professor, Canada Excellence Research Chair and Associate Director
Address	Global Institute for Food Security, University of Saskatchewan 421 Downey Road, Suite 101, Saskatoon, SK S7N 4L8
Phone	Office: 306-966-3712
Email	Leon.Kochian@usask.ca

Project contributors:	**Céline Ferré** (M.Sc. Student); **Xuan Yang** (Technical Officer); **Michael Taylor** (M.Sc. Student); **Shengjian Ye** (Technical Officer); CDC Oat Breeding Group.

4. Abstract (Not more than 250 words). *Describe in lay language progress towards project objectives over the last reporting period. Include any key findings, interim conclusions and any deviations from the original methodology.*

Lodging is a significant issue in oat and assessment of root and stem traits important for lodging resistance will provide critical knowledge for the development of cultivars with improved standability. During 2022, field trials of 14 oat lines in Saskatoon, Kernen and Codette and assessed for stem traits, leaf angle, plant height, and panicle architecture. Root crowns were excavated and assessed for root angle, spread, and structural depth. To date, field traits associated with lodging include plant height, second-internode length, inner stem diameter, and flag leaf angle. Lodging resistant oat genotypes such

as AC Morgan and OT3071 had consistently larger stems across field environments. Increased seeding rate was associated with decreased stem strength, outer diameter and thickness. Initial results from indoor root phenotyping of 22 oat lines showed a lack of variation in seminal angle, which is in contrast to barley where seminal angle variation is highly correlated to lodging resistance. Median root number and number of root system holes, related to root branching complexity, were associated with lodging resistance in oat. Screening of additional diverse oat lines revealed considerable variation in overall root architecture and seminal angle. Preliminary screening in rhizoboxes demonstrated association of root system spread with lodging resistance. As 2023 field trials proceed, the project will continue to investigate how stem traits and flag leaf angle are related to lodging. Continuing to characterize root architectural variation across western Canadian and global germplasm will be important as we establish which root traits are critical for oat lodging resistance.

5. Introduction: *Brief project background and rationale (**Maximum of 1500 words or 1.5-3 pages).***

Brief project background and rationale.

The ability of crops to maintain mechanical stability and support through contrasting environments with increased winds and heavy precipitation is critical for reaching yield potential and successful production outcomes (Gardiner et al. 2016). Mechanical failure of a crop, or lodging, is the permanent displacement of plants from their normal vertical growth position (Shah et al. 2017). Lodging of cereal crops is of considerable significance, leading to yield reductions and major economic losses and is a high priority for plant breeders worldwide (Reynolds et al. 2008; Baker et al. 2014).

To build on Saskatchewan's (and Canada's) position as a supplier of premium quality oat to current U.S. markets and developing markets in Mexico and China requires developing varieties with improved traits, including better lodging resistance. This will provide value to oat growers through prevention of yield losses (Marshall et al., 1986) and improved harvestability by avoiding the need to pick up a lodged crop which adds expense to farm operations (Berry et al., 2004). Additionally, a standing crop maintains both physical and nutritional quality and accumulates less disease on the grain. May et al. (2004) observed lower grain test weight, plumpness and groat percentage when nitrogen rate, and thus lodging, increased in a lodging-prone variety. Furthermore, a positive correlation between lodging incidence and severity of mycotoxin contamination was reported among a set of European oat varieties (Kuchynková and Kalinová, 2021) with approximately twice as much Fusarium-produced DON mycotoxin detected in grain from oat plots that had lodged compared to non-lodged plots (Langseth and Stabbetorp, 1996).

Plant lodging is divided into two types, root lodging and stem lodging (Berry et al., 2003). Stem lodging or stem buckling occurs when a stem breaks or is otherwise compromised by external mechanical forces (Berry et al., 2003). Root lodging occurs when shoot-derived forces exceed the capacity of the root system to anchor the plant and results in the rotation or movement of the root system in the soil thereby leading to anchorage failure (Ennos, 1991).

Lodging most often occurs due to the combined effects of heavy wind and rain but is also influenced by other factors including agronomic practices and soil nutrition. Increased lodging was reported in oat when nitrogen rates reached 84 kg/ha (Brinkman and Rho, 1984) to 100 kg/ha (May et al., 2020), the rate at which lodging occurred being influenced by the oat variety used. Marshall et al. (1986) observed a linear increase in lodging in the variety 'Ogle' as seeding rate increased from 18 to 36 plants/ft^2. The effect of seeding rate may be dependent on oat variety. Increased seeding rate led to higher lodging for prostrate leaf-type varieties, but not for erect leaf-type varieties (Wu and Ma, 2019). A major

determinant in oat lodging can be the larger drag area created by panicle interlocking between different plants and this may be a reason why oats require stronger stems relative to other cereals such as wheat (Mohammadi et al., 2020). Thus, an erect-leaf growth habit emphasizes lower inter-plant competition (Li et al., 2018) and, arguably, less panicle interlocking which may explain less lodging in erect varieties. Oat plants are often more prone to root anchorage failure than other small cereal grains such as wheat (Wu and Ma, 2019; Mohammadi et al., 2020). However, the contribution of root traits to oat lodging has not been investigated to the extent it has in other cereals but there are clear mechanistic correlations to other species including the importance the horizontal spread of the root system. Early research in the 1960s identified larger root-crowns, larger root-diameters, and lower shoot-to-root ratios as important to oat lodging resistance (Sechler, 1961). In oat, modeling of lodging indicates that root plate diameter along with drag area contributed by panicle interlocking were the most influential to root lodging (Mohammadi et al., 2020).

The interaction between oat variety, growth habit, and seeding rate on lodging risk underscores the importance that genetics have on lodging. For example, a wide range in lodging was observed in a diverse set of European germplasm that included both new and old varieties and a number of landraces (Tumino et al., 2017). One of the most important traits associated with lodging resistance is plant height. Several studies have observed a correlation between increased plant height and tendency for lodging to occur (Buerstmayr et al., 2007; Tumino et al., 2017). Conversely, when plant height is reduced through application of plant growth regulators the severity of lodging is reduced (Aidoo, 2017). The introduction of dwarfing genes in cereals such as wheat and rice resulted in decreased lodging risk and significantly increased yields through improved biomass partitioning towards the grain (Hedden, 2003). However, unlike rice and wheat, the introduction of the dwarf trait in oat not only caused shortened internodes (and height) but also significant reductions in panicle length and overall grain yield (Milach, 1998; Molnar et al., 2012). While progress to offset the negative yield impacts of dwarfing genes in oat has occurred, it should be noted that the reduction in height does not always lead to increased lodging resistance when compared to tall non-dwarf cultivars (de Rocquigny et al., 2004).

Summary

Growing markets for oat (*Avena sativa* L.) are providing opportunities for growers to make oat a more economically viable crop within rotations. Lodging and mechanical failure of the stem or root anchorage system is a significant issue for oats leading to yield reductions and economic losses for Canadian producers. Development of oat varieties with improved lodging resistance is thus a high breeding priority. Assessment of root and stem traits important for lodging resistance will provide critical knowledge required for development of cultivars with high standability. The project will utilize a suite of innovative root imaging systems to characterize root system architecture in relevant Canadian oat germplasm and, furthermore, incorporate analyses of stem strength and root anchorage from Prairie field environments. Plant growth habit and panicle architecture will also be analyzed as this has been associated with lodging in oat. The combined assessments using high-throughput imaging and biomechanical strength testing will define root and stem traits that are critical for lodging resistance – thus, laying the groundwork for incorporating robust standability traits into future western Canadian varieties. A second objective of the project is to assess RSA in a larger and more diverse set of oat genotypes to understand root trait diversity and potentially identify oat germplasm with more favourable root traits. Defining the root architecture traits within this larger set of germplasm will be a valuable resource for breeding lodging resistant cultivars and possible future studies related to nutrient uptake or abiotic (drought/salt) stress tolerance.

6. Objectives and the *progress towards meeting each objective:*

Please list the original objectives or revised objectives if Ministry-approved revisions have been made. A justification is needed for any deviation from original objectives. Note progress, completed or in progress.	
Objectives	**Progress**
1. Evaluate root system architecture in oat cultivars which vary in lodging resistance.	*In Progress (80%) – Indoor controlled environment root phenotyping.* Seminal root angle and 2D pouch phenotyping at seedling stages have been completed for 22 oat genotypes varying in field lodging resistance. Rhizobox phenotyping assessing root architecture through to oat maturity has been completed for 8 of the 22 oat genotypes with experiments ongoing. Data analysis for 24 traits related to root system topology, size, and individual root traits, was completed for the seminal angle and 2D pouch phenotyping and revealed smaller than expected variation in root traits usually associated with lodging resistance (e.g., root system width and defining traits such as seminal angle). We diverted project resources to Objective 5 to begin evaluating root trait variation in a set of diverse oat genotypes. Overall, this objective is on-track to complete a rubust evaluation of root system architecture (RSA) for the 22 oat genotypes in 2023. Significant traits associated to lodging have been noted with follow-up analyses on-going. Additional root phenotyping methods (e.g., 3D RSA, crown-root assessments) will be added as necessary. Genotypes of focus for more detailed phenotyping may include a subset of diverse RSA phenotypes discovered through Objective 5.
2. Evaluate stem and root lodging in field trials.	*In Progress (50%) – Field trials assessing lodging-related traits.* In 2022, field trials were grown as 3 replicate randomized completed block designs at 3 sites, Saskatoon, Kernen and Codette, and assessed for field traits and lodging. An additional site was grown at Brandon that was used to assess lodging only. Little to no lodging was observed in 2022. Measurements of stem, root, and agronomic traits were completed for year 1 trials and panicles were collected at 2 sites for imaging and analysis. The second year of field trials to measure stem and root traits are underway at Saskatoon, Kernen, Codette and Brandon. Preliminary analysis of year 1 data has been completed including the generation of best linear unbiased prediction (BLUP) values, data normalization, and significance and correlation analyses. In total, 33 traits representing stem, root, agronomic, and panicle architecture were collected for preliminary analysis. Significant traits associated to lodging have been discovered with a more thorough investigation to be accomplished after the second year of field data has been collected.
3. Assess impact of seeding rate on key stem and root lodging-related traits in field trials.	*In Progress (50%) – Seeding rate impacts on lodging-related traits.* Seeding rate trials were completed at 2 sites, Saskatoon and Codette, in 2022. Replicate trials for 2023 are underway. Trials in 2022 consisted of testing 4 oat genotypes under 3 seeding rates to assess the impact of seeding rate on stem and root traits which are related to lodging. In

	total, data for 18 stem and root traits was collected; panicles were collected at Codette for imaging and analysis. Premlinary data analysis has been completed for year 1 including significance and correlation analyses. Increased seeding rate, which usually results in increased lodging, has been associated with decreased stem strength.
4. Assess the correlation between various root phenotyping methods to develop a robust trait selection pipeline for breeding application.	*In Progress (10%) – Phenotyping method for oat breeding application.* Progress on this objective has been delayed as we pivoted to begin Objective 5 early. It is necessary to make sure we establish the variation for root traits present in both western Canadian germplasm and diverse global oat accessions. This will help establish which root traits are most important to lodging resistance and those with the greatest potential for breeding selections. This objective may also expand to include relevant stem traits that are important to lodging resistance. The objective is still on-target for completion in 2024.
5. Compare root system architecture between Canadian oat germplasm and a diverse set of oat germplasm.	*In Progress (35%) – Evaluate root architecture in a collection of diverse oat accessions.* Started objective early, in April 2023, to explore additional variation in oat germplasm. To date, 50 oat genotypes have been imaged at 3, 7, 10, and 14 days following germination. Seminal root angle measurements at 3 and 7 days have been completed for 34 genotypes with significant variation discovered. Significant visual differences in root system architecture have also been observed with image analyses pending in the coming months. Anticipated that root phenotyping and image analysis of the CORE collection of 113 oat genotypes will be completed in 2023; originally this objective was planned for the last year of the project (2024-25).

7. Changes in the work plan, or budget:

Briefly explain new challenges found during the work completed in this reporting period and the impact on the work plan or the budget ***(Maximum of 1 page)***

No significant challenges during the reporting period. As noted above:

- Objectives 2 and 3: In 2022 little to no lodging was observed. We hope to collect robust numerical lodging ratings in 2023 from some of the 4 sites being used. In addition, a second trial has been established at Codette that is being grown under higher fertility conditions in an attempt to promote lodging. This will be important for the discovery of lodging-related traits and development of trait models for lodging resistance.
- Objectives 1, 4, 5: As a result of the lack of variation in root traits related to lodging in the 22 oat lines initially profiled, we subsequently pivoted to start Objective 5 early. Profiling of additional oat lines has revealed significant variation in traits such as seminal root angle. Further, assessments of mature root systems of a subset of the 22 oat lines have revealed the potential impact of root system spread on lodging resistance.

8. Methodology:

Specify project activities undertaken during this reporting period. Include approaches, experimental design, tests, materials, sites, etc. Please note that any significant changes from the original work plan will require written approval from the Ministry. ***(Maximum of 5 pages)***

Oat Genotypes

The four experiments accomplished to date, representing project objectives 1, 2, 3, and 5, each utilized a different set of oat genotypes listed in Appendix 1 – Tables 1 and 2. Twenty-two (22) oat genotypes were used for Objective 1 and evaluation of root system architecture in indoor controlled environment experiments. These 22 genotypes capture a selection of North American and European germplasm adapted to western Canada and range in field lodging resistance and plant height. For Objective 2, fourteen (14) of the 22 genotypes were utilized in field experiments to assess root, stem, panicle, and agronomic traits related to lodging resistance. Four (4) of the 14 genotypes were used for Objective 3 to test the impact of seeding rate lodging-related traits. For Objective 5, to further explore and exploit root trait variation in oat, a diverse collection of 113 oat accessions are being evaluated in controlled environments to assess differences in seminal root angle and 2D root system architecture. The 113 oat accessions compose the world diversity panel assembled by the Collaborative Oat Research Enterprise as part of its efforts to increase the genetic resources available to oat breeders and researchers, including the creation of high-throughput marker technology and a new consensus map (Klos et al. 2016).

Field Trials

Oat-1 Trial Assessing Lodging-Related Traits and Oat-2 Trial of Seeding Rate Impacts

Oat-1 Trial Design

Field trials were conducted in the summer of 2022 at 4 locations using a three-replicate randomized complete block design. Trial locations were Crop Science Seed Farm (irrigated) and Kernen Crop Research Farm (dryland), both located in Saskatoon, SK, as well as the Discovery Ag Research Farm located in Codette, SK and the AAFC-Brandon Research and Development Centre farm in Brandon, MB. All plots had a seeding rate of 300 plants/m^2. The Brandon site was used to collect lodging data, while the three Saskatchewan locations were used to collect lodging data, agronomic data, as well as plant, stem and root traits potentially relevant to lodging.

Oat-2 Trial Design

Field trials were conducted in the summer of 2022 at two locations using a three-replicate two factorial experiment in a randomized complete block design. The factors consisted of four genotypes and three seeding rates. The seeding rates consisted of 300 plants/m^2 (standard rate), 200 plants/m^2 (low rate) and 400 plants/m^2 (high rate). Trial locations were the Crop Science Seed Farm (irrigated), located in Saskatoon, SK, as well as the Discovery Ag Research Farm located in Codette, SK.

Whole Plant Data Collection

Agronomic data collected included plant height, days to flowering, days to maturity and yield. When no lodging was observed in field trials lodging ratings were assigned to genotypes based on historical information. Lodging categories of very good, good, fair, and poor were converted to a scale of 1 to 10, with 1 being no lodging and 10 being fully lodged. Using this scale categories were converted as follows: very good = 2, good = 4, fair = 6 and poor = 8. Once plants reached Zadoks Growth Stage 75 to 85 (mid-milk to soft dough), leaf angle was measured. Five main stems were chosen at random

from the three middle rows of the plot and angle was measured between the base of the leaf and the inside of the stem for each of the top three leaves on each stem. Stem bending resistance (or force) was measured on a 1-meter section within one of the three inner rows of the plot using the Stalker. The Stalker crossbeam was placed at half the plot's average height. The Stalker crossbeam is connected to a load cell that collects the angle and force along the Stalker's entire movement path once turned on, and the maximum force was extracted. The section used to measure stem bending resistance was marked and plant counts and panicle counts were recorded.

Stem Data Collection

Five plants were cut at the soil from within the same section used to measure stem bending resistance and a 3-point bend test was conducted on the second internode of the main stem to determine stem strength. Force was applied using a custom 3-point bend test machine (constructed by Dr. Scott Noble, University of Saskatchewan; Fig. 1) until breakage occurred. The peak applied force was extracted and used as the estimate of stem strength. Using this data stem failure was calculated using the following equation:

$$B_S = F_S * h/4$$

Where B_s is stem failure, F_s is the internode breaking strength (i.e. stem strength), and h is the internode length in mm. The following equations were used in the calculation of bending moment at breaking (BMB), cross section modulus (SMOD), and bending stress (BST):

$$BMB\ (gf \cdot mm) = F\ x\ L\ /\ 4$$

$$SMOD\ (mm^3) = \frac{\pi\ (OD^4 - ID^4)}{32\ OD}$$

$$Bending\ Stress\ (gf \cdot mm^{-2}) = \frac{BMB}{SMOD}$$

Where: OD = outer stem diameter (mm); ID = inner stem diameter (mm); F = bending force (gram-force, gf); L = distance between supports, 100 mm (Duy et al., 2004; Ookawa et al., 2016).

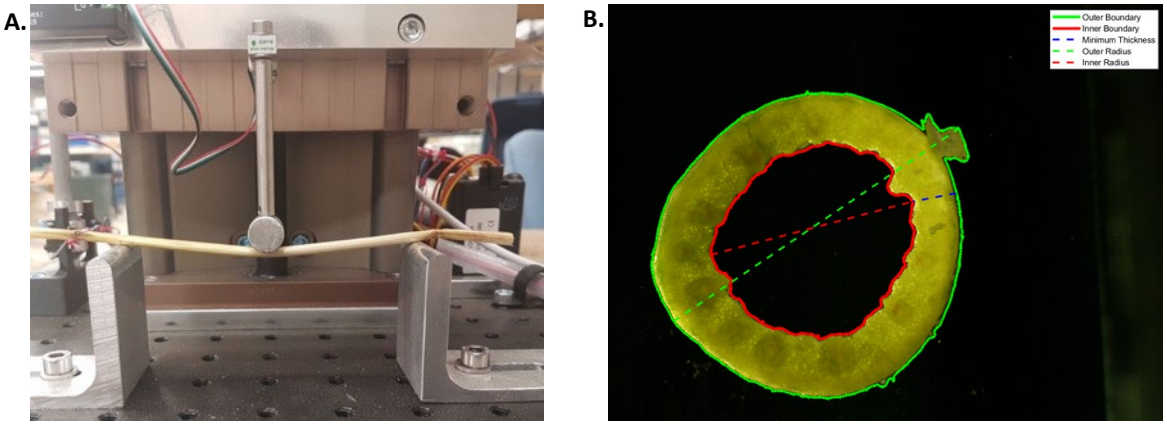

Fig. 1. (A) The 3-point bend test machine used to determine stem internode strength. (B) Example of processed stem cross-section image. The solid green line represents the outer stem wall, the dashed green line represents the outer stem diameter, the solid red line represents the inner stem wall, the dashed red line represents the inner stem diameter, and the dashed blue line indicated the stem wall thickness.

After the 3-point bend test was completed a 1 mm cross-section was cut from the same internode and imaged using an inverted 18MP USB 3.0 Real-Time Live Video Microscope Digital Camera connected to an Amscope stereo microscope. Images were processed using custom software (R. Peters, University of Saskatchewan) to measure the minimum stem wall thickness, maximum inner stem diameter and maximum outer stem diameter. An example of a processed stem image can be seen in Fig. 1.

Root Data Collection

The root systems of the 5 plants used in the 3-point bend tests were excavated using shoveling. Roots were soaked in water-filled tubs for 15-30 min to aid in removal of adhering soil followed by measurement of maximum crown root angle, root plate spread, and root plate depth (Fig. 2). Following measurement of crown root angle, root plate spread, and root plate depth the roots were taken to the NRC for imaging using a Canon 7D DLSR. Images were then analyzed using ImageJ (Schneider et al. 2012) to measure root angle and RhizoVision Explorer (Seethepalli *et al*., 2021) to extract additional root features.

Fig. 2. An excavated oat root system obtained by shovelomics. The red vertical line represents the root plate depth, the yellow line represents root plate spread and the white angle at the top represents the root plate angle.

Panicle Analysis

Panicles were collected from 2 field sites in 2022, Codette and Kernen, and imaged with a Canon 7D DLSR camera. Images were segmented and analyzed in Rhizovision Explorer and ImageJ following the procedure for roots. Six panicle traits were initially documented: Bottom Branch Angle, Convex Area, Panicle Area, Height, Width, and Width-to-Depth Ratio.

Statistical Analysis

All statistical analyses were completed using the R statistical computing language (R Core Team, 2021) in the RStudio development environment (RStudio Team, 2020). The R packages dplyr, tidyr, purrr, lmerTest, broom.mixed, ggplot2, and ggcorrplot were used for analyses described below (Kuznetsova 2017; Wickham et al. 2019; Bolker and Robinson, 2021; Kassambara 2022). The effect of genotype, location and genotype by location interaction on all field traits were analyzed as a RCBD using a linear mixed effect model in the lmer function. For the Oat-1 trial, genotype was treated as a fixed effect while location and genotype by location were treated as random effects. For the Oat-2 trial, the linear mixed model included genotype, location, seeding rate, genotype by location interaction and seeding rate by genotype interaction as factors. Genotype and seeding rate were treated as fixed effects while location and genotype by location were treated as random effects. The

assumptions of homogeneous variances and normal distribution of residuals were evaluated using plots of predicted values versus residuals and the Shapiro-Wilk test, respectively. Pearson correlation matrices were generated using the rcorr function in the R-package hmisc to evaluate interactions among all traits measured. Data used for correlation analysis consisted of best linear unbiased predictions (BLUPs) calculated for each genotype-trait combination on a location basis (due to the significant effect of location on traits) followed by z-scaling to account for differences in the range of trait values across locations. Broad-sense heritability was calculated in R for all traits using the following equation:

$$H^2 = 1 - \frac{\bar{v}_{\Delta}^{BLUP}}{2\sigma_g^2}$$

Where $\bar{v}_{\Delta}^{BLUP}$ is the average BLUP difference, σ^2 is the variance, and g is genotype, as described by Cullis *et al*. (2006). Description of trait abbreviations used in this study are listed in Appendix 1.

Root System Architecture Experiments in Controlled Environments

Seminal root angle, 2-dimensional (2D) hydroponic pouch and rhizobox experiments were carried out on all genotypes listed in Table 1. All lab-based experiments occurred in a controlled-environment growth chamber under the following conditions: 16-hour photoperiod, 22ºC day, 18ºC night, and a light intensity of 270 µmol/m^2/s.

Seminal Root Emergence Angle

Oat grain was treated with 0.5% (v/v) of Maxim Quattro Seed Treatment (Syngenta) at a ratio of 40 µL per gram of grain and dried on seed aging trays. Treated seeds were placed onto moistened filter paper in a Parafilm-sealed Petri dish and incubated at 4°C for 4-5 days to help synchronize germination. After cold-treatment, seeds were transferred to a germination pouch system. Each pouch consisted of a polyethylene file-folder (28.5 x 23.5 cm) and one piece of brown germination paper and one piece of black filter paper in-between. Within the file folder, six oat grains were placed on wetted black filter paper 2 cm from the top edge with the embryo-side facing down; wetted germination paper was placed to cover the grains. The pouches were suspended in a polypropylene tank with the bottom 5 cm of the pouch submerged in distilled water and the container covered. Tanks were placed in a growth chamber for germination and images of the seminal root system were after 4 days using a Nikon D850 DSLR with StrobePro 600W lighting system and analyzed using ImageJ (Schneider et al. 2012). This experiment took place over 3 rounds, with two pouches for each genotype in each of the 3 sub-experiments.

2-Dimensional (2D) Hydroponic Pouch

Four days following germination, uniform seedlings were transferred to individual growth pouches. Each pouch (40.5 x 40.5 cm) included (from bottom to top layer): a perforated polypropylene plate, three layers of brown germination paper, one layer of black filter paper, one oat seedling, and a transparent polyester sheet. The 2D pouches were suspended in a polypropylene tank, which was filled with the bottom 5 cm of the pouch submerged in nutrient solution. Nutrient solution was subsequently added to fully submerge the pouches at 1.5-hour intervals to ensure the pouches remained saturated throughout the entirety of the experiment. The nutrient solution was a modified Magnavaca solution (Magnavaca et al. 1987) comprised of: 3.5 mM $Ca(NO_3)_2$, 1.3 mM NH_4NO_3, 0.5 mM KCl, 0.5 mM K_2SO_4, 0.5 mM KNO_3, 0.8 mM $Mg(NO_3)_2$, 0.2 mM KH_2PO_4, 0.08 mM Fe-HEDTA, 9 µM $MnCl_2$, 25 µM H_3BO_3, 2.3 µM $ZnSO_4$, 0.6 µM $CuSO_4$, and 0.8 µM Na_2MoO_4. The pH of the solution was adjusted to pH 5.6 using KOH and nutrient solution was changed weekly. Individual pouches were imaged using a Nikon D850

DSLR with StrobePro 600W lighting system at 10-, 14-, and 17-days after germination (Zadoks Growth Stages 11, 12, and 13, respectively) (Zadoks et al. 1974). This experiment took place over 3 rounds, with 4 pouches for each genotype in each round, resulting in twelve total plants per genotype. Images were analyzed using Rhizovision Explorer (Seethepalli *et al*., 2021) with the root traits assessed documented in Appendix 1.

Modifications for Seminal Angle and 2D Pouch Hydroponics

For the CORE oat diversity collection root screening, an updated procedure for seminal angle and 2D root phenotyping was utilized that eliminated the transfer step to individual growth pouches. While this results in less seminal angles being measured, it ensures that root growth remains consistent through the overall process to assess root architecture from early germination through to seeding and plant establishment. The modified experimental workflow includes germination directly on growth pouches and selection of 6 uniformly-germinated seedlings at 4 days following germination for follow-up 2D seedling root imaging. In addition, the interval between flooding of the hydroponic tank to saturate the pouches with nutrient solution has been increased to 4 hours as we found this produced more realistic root system growth and faster overall plant growth. Seminal angle was measured at 3 days following germination which represents Zadoks stage 09 (First green leaf just at tip of coleoptile; Zadoks et al. 1974). 2D imaging time points were at 7, 10, and 14 days following germination which are equivalent to Zadoks stage 11 (First leaf emerged), Zadoks 12 (Two leaves emerged) and Zadoks 13 (Three leaves emerged). Seminal angles were also measured at 7 days and root architectural assessments were performed in Rhizovison Explorer as detailed above.

Rhizobox

Rhizoboxes were used to observe root growth throughout oat development in a soil-like medium through the use of transparent acrylic panels measuring 60 x 0.6 x 80 cm (length x width x height). Two uniformly germinated seedlings, prepared in the same manner as for the 2D hydroponic pouch experiments, were transplanted to a rhizobox and planted about 4 cm deep. Six oat plants were evaluated for each genotype and eight genotypes were grown in one experiment with two genotypes in common between each set of experiments to measure variability. Rhizoboxes were constructed by placing pre-wetted soil-less potting medium (e.g., Sun Gro Perlite-Free Mix RESILIENCE) between two transparent acrylic panels which were wrapped in non-transparent plastic sheets to prevent light penetration. Rhizoboxes were inclined to 45° (from the horizontal plane) so that roots could grow predominately along the bottom panel. Root systems were scanned at 2-, 3-, 7-, and 11-weeks after germination using a large format flatbed scanner (Kurabo K-IS-A1FW Flatbed). Images were analyzed using Rhizovision Explorer (Seethepalli *et al*., 2021) with root traits assessed listed in Appendix 1.

Statistical Analysis

Statistical analyses for the 2D pouches were completed in the same manner as described in Study 1 except the linear mixed model included genotype and round. Genotype was treated as a fixed effect and round was treated as a random effect. Best linear unbiased predictions were generated using the R package lmerTest (Kuznetsova et al. 2017) with the equation:

$$Trait = (1|Genotype) + (1|Experiment) + (1|\text{Genotype: Experiment})$$

where genotype and experiment were treated as random effects. Data was mapped over each trait and summarized using the R packages dplyr, tidyr, purrr, and broom.mixed (Wickham et al. 2019; Bolker and Robinson, 2022;). Graphs, except scatterplot matrices, were produced using the package ggplot2 (Wickham et al. 2019); scatterplot matrices were built from code in the PerformanceAnalytics package

(Peterson and Carl 2020). Graph colours were selected using the pals package (Wright 2021). Correlation graphs were produced with the ggcorplot package (Kassambara 2022). For some datasets, preliminary data arrangement and summary occurred in Microsoft Excel. PDF figure files from R were arranged in Adobe Illustrator CC. Adobe Photoshop CC and Adobe Illustrator CC were used to arrange images.

9. Results and discussion:

Describe research accomplishments during the reporting period under relevant objectives listed under section 6. The results need to be accompanied with tables, graphs and/or other illustrations. Provide discussion necessary to the full understanding of the results. Where applicable, results should be discussed in the context of existing knowledge and relevant literature. Detail any major concerns or project setbacks. ***(Maximum of 20 pages of text not including figures or tables).***

9.1 Differences in root system architecture traits in a set of 22 oat genotypes

Screening of seminal root angle (i.e., the angle between the growth paths of the outer most seminal roots) revealed differences between 69 and 45 degrees with AC Nicolas (a cultivar with good lodging resistance) and OT3098 (a semi-dwarf breeding line with very good lodging resistance) displaying the highest and lowest seminal angle, respectively. However, if we account for the experimental variation between experiments and generate best linear unbiased predictions (BLUPs), then the range in seminal angle observed decreases to between 65 and 50 degrees with AC Nicolas and OT3098 remaining as the genotypes with highest and lowest seminal angle at 4-days after germination (Fig. 3). Overall, there was limited variation in seminal angle within the 22 oat genotypes profiled and there was no significant correlation of 4-day seminal angle to lodging rating (Figs. 3 and 4). This is in contrast to barley where screening of seminal angle in 12 cultivars varying in lodging resistance displayed a range between 86 and 38 degrees in 3-day seminal angle measurements and a Pearson correlation to lodging rating of -0.77 ($p < 0.01$) (results from ADF20190282 project). Thus, we concluded that in the western Canadian oat genotype set, emergence of early seminal roots do not correlate with lodging resistance. This is not the end of the story however. As demonstrated below in Section 9.2, screening of the diverse oat genotype set revealed significant variation in seminal angle and importantly it was found that emergence of later seminal roots occured at wider angles that were not consistent with early seminal root angle. Thus, we are currently following up with further assessments of seminal angle at later developmental stages in the set of 22 oat genotypes.

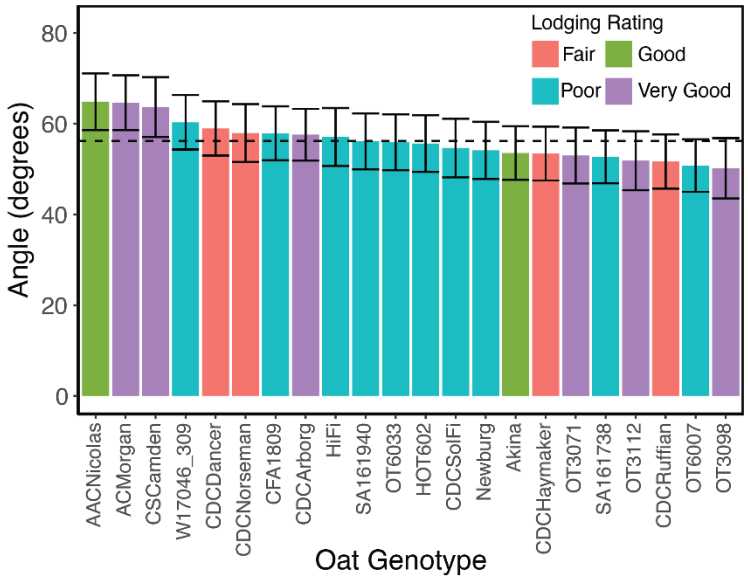

Fig. 3. Seminal root angles of 22 oat cultivars and breeding lines with varying lodging resistance. Measurement represents angle between outermost seminal roots at 4 days following germination. Error bars are the 95% confidence interval of best linear unbiased prediction (BLUP) for each genotype. Dotted line represents overall mean BLUP seminal angle of 56 degrees.

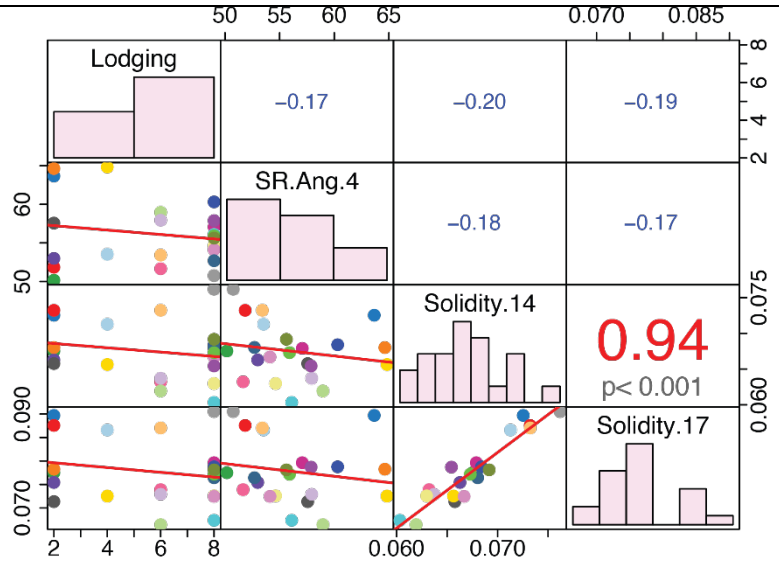

Fig. 4. Root traits such as seminal angle and root system solidity (the ratio of network area to the convex area the root system occupies) have been associated to lodging resistance from our work in barley but do not have relationships to lodging in oat. Seminal root angle at 4 days following germination (SR.Ang.4) and root system solidity at 14 and 17 days (Solidity.14; Solidity.17) were measured on 22 oat genotypes relevant to western Canada and representing a range of lodging resistance. Lodging values were converted to numerical values based on ratings (e.g., very good = 2; good = 4; fair = 6; poor = 8).

Following measurement of seminal angle, root imaging was performed on 10-, 14-, and 17-day-old seedlings (Fig. 5). To date, root system trait analysis has been accomplished for 14- and 17-day seedlings measuring a range of root traits representing root system topology (e.g., root width to depth ratio, solidity, convex area), biomass (e.g., network area, volume), and individual root traits (e.g., root diameter) (see Appendix 1 – Table 3 for trait descriptions). In total, 23 root system traits were measured (Appendix 1, Figs. 1 and 2). There were distinctive cultivar differences across various traits. For example, in 17 days seedlings the root systems of AC Morgan and CDC Arborg covered the largest area and had the widest root systems while HOT602 and CDC Ruffian covered the smallest area with less root biomass (e.g., total length) and had the narrowest root systems. In terms of overall root biomass (area / volume / total length), OT6007 was the highest but was a more compact root system with the highest solidity and roots per unit area. For average root diameter, CDC Norseman and AC Nicolas were thinnest and HOT602 and CS Camden were widest.

In terms of 2D root traits related to field lodging resistance, in barley we have found that root system solidity (the ratio of network area to the convex area which the root system occupies) is highly related to lodging. The more spread out a root system, particularly in terms of width, the greater the lodging resistance. This is consistent with the literature defining root plate spead (the width of the root system in the upper soil layers) as being important to lodging resistance in cereals such as wheat, barley, and oat (Berry et al. 2003; Berry et al. 2006; Mohammadi et al. 2020). In barley, we found that solidity was correlated to field lodging (r=0.7) and negatively correlated to 3-day seminal root angle (r=-0.7). In the 22 oat genotypes profiled, solidity was not correlated to 4-day seminal root angle or to lodging (Fig. 4).

Root traits which were significantly correlated to field lodging ($p < 0.05$) included median root number and the number of root system holes (Fig. 6). The number of root system holes is highly correlated to median root number ($r = 0.75$-0.91, $p < 0.001$) and represents overall root branching and complexity.

Conceivably, a greater number of root branches could promote root anchorage in oat and potentially lodging resistance. These traits will be further evaluated as the project proceeds.

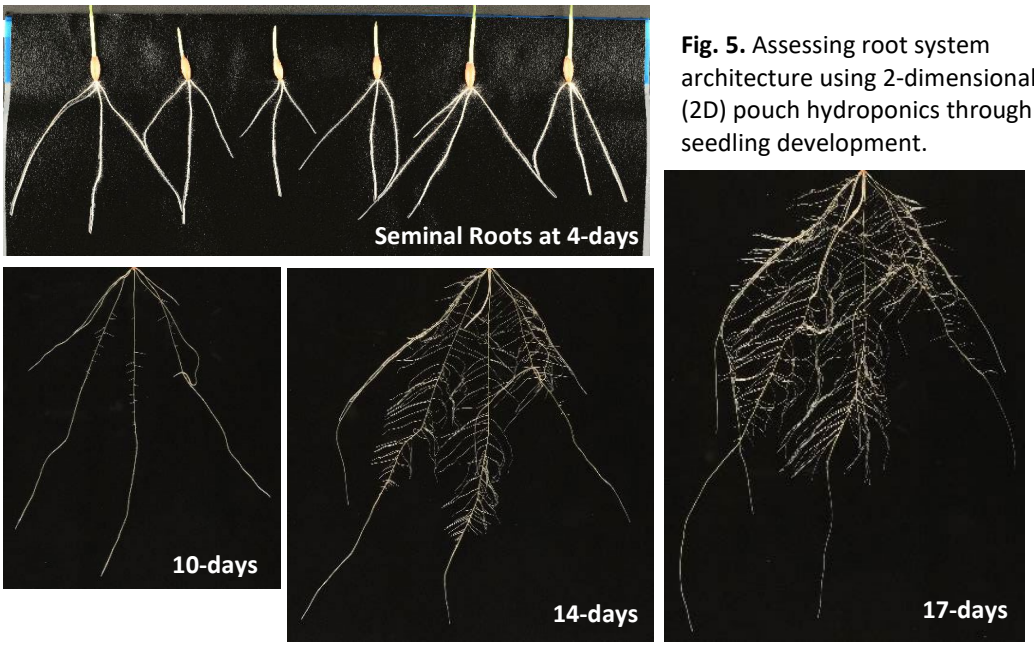

Fig. 5. Assessing root system architecture using 2-dimensional (2D) pouch hydroponics through seedling development.

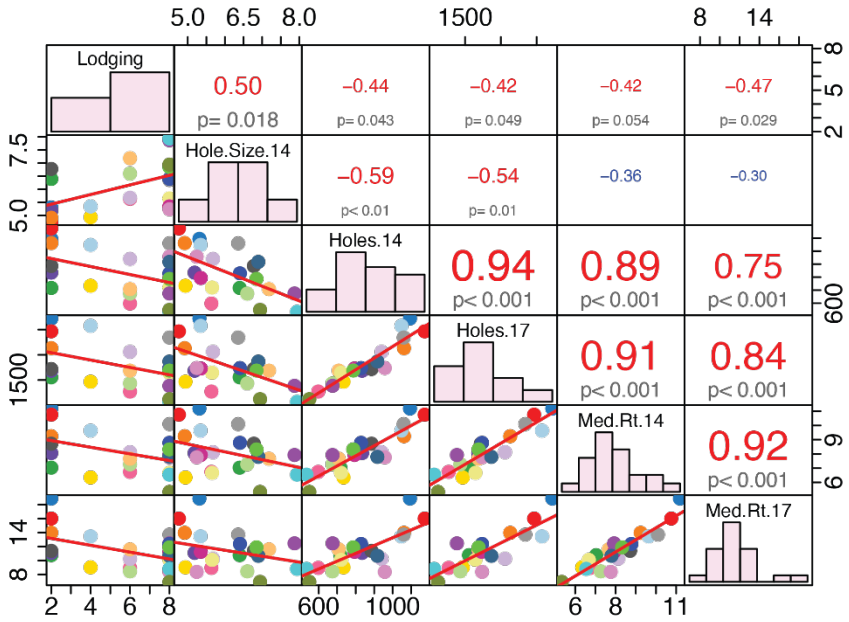

Fig. 6. Root system traits significantly correlated to field lodging rating as calculated by Pearson correlation coefficient ($p < 0.05$). Average lodging rating (see Fig. 4) compared to root hole size (Hole.Size.14), the number of root system holes (Holes.14 ; Holes.17), and median root number (Med.Rt.14; Med.Rt.17) (see Appendix 1 – Table 3 for trait descriptions). Pearson correlation coefficients are displayed in the upper panel with p-values, histograms displayed on the diagonal, and linear regressions displayed in lower panel point graphs.

Rhizoboxes were used to assess oat root systems through development. To date, we have completed imaging of 8 of the 22 oat genotypes. Early results are promising, with oat genotypes with contrasting lodging resistance displaying different root phenotypes (Fig. 7). For example, CDC Arborg has wider root system angles which drives greater spread of the root system in the upper soil layers and may explain why this variety has very good lodging resistance. In contrast, OT6033 has narrower root system angles and, thus, perhaps explains why it has poor lodging resistance. As the rhizobox imaging and analysis of the 22 oat genotypes is completed in the coming months it will be interesting to observe how mature root system angles may be associated with oat standability in other cultivars and breeding lines.

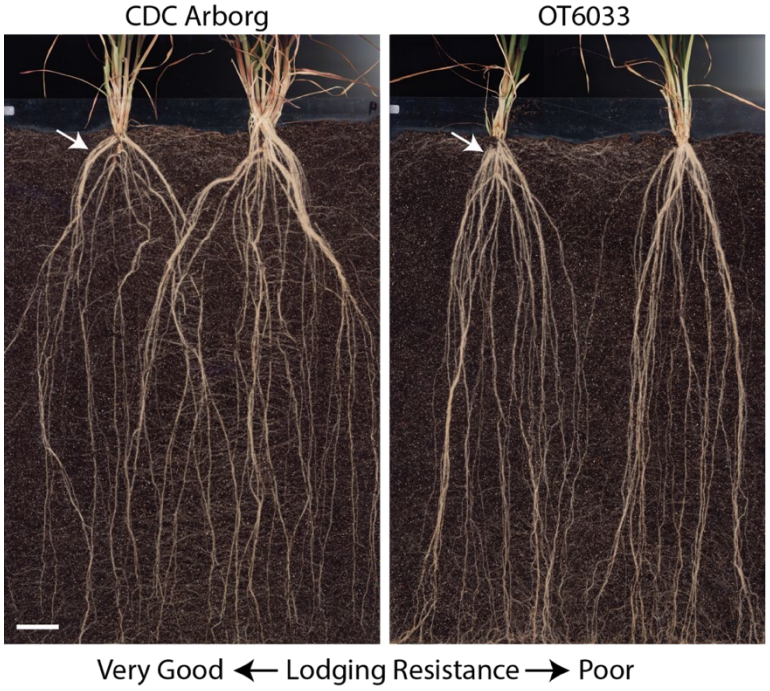

Fig. 7. Rhizobox oat root system images captured 11 weeks following germination of cultivar CDC Arborg and breeding line OT6033. Note the wider root angles of especially the crown roots (arrows) in lodging resistant CDC Arborg compared to lodging susceptible OT6033. Scale bar (lower left) represents 6 cm.

9.2 Assessment of root system architecture traits in a collection of diverse oat genotypes

To further investigate the variation present in root architectural traits, the screening of an oat diversity panel was initiated. The CORE collection of oat genotypes represents the world diversity panel assembled by the Collaborative Oat Research Enterprise. It includes accessions from North America, South America, Europe, Australia and Asia with both modern cultivars and historically relevant landraces. To date, we have performed root imaging for 50 of the 113 oat accessions present in the collection. The images represent 3-, 7-, 10-, and 14-day old oat seeding root images which will be analyzed for seminal root angles and various 2D root traits (see Appendix – Table 3 for trait descriptions). While completion of analyses are still to be accomplished, it is evident that there is considerable root system variation present in the genotypes imaged to date (Fig. 8).

We proceeded to measure seminal root angle at both 3- and 7-days following germination. Interestingly, in oat there were new seminal roots which emerged from the grain between 3- and 7-days with greater angles than those roots which emerged at the time of germination (Fig. 9ab). The new seminal root angle measured at 7-days was only weakly related to the 3-day seminal root angle (R^2

= 0.15; Fig. 9c). This discovery, along with the building of our knowledge base for root system diversity in oat, will move us forward in terms of building the foundation necessary to identify which

Fig. 8. Oat root system images captured 14 days following germination from the 2D pouch hydroponics workflow. Images represent the 34 accessions imaged to date from the oat CORE germplasm diversity panel.

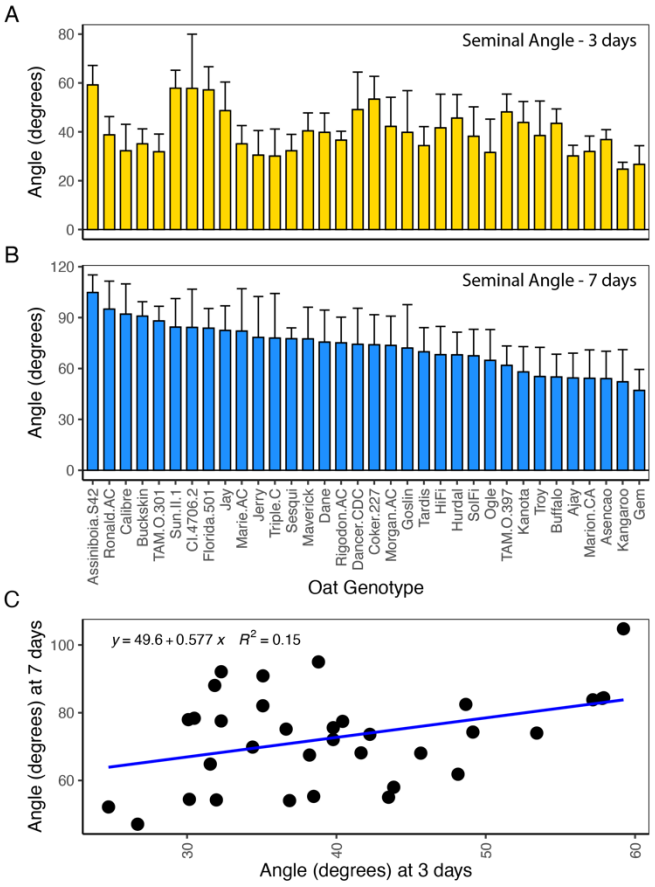

Fig. 9. Seminal root angles of 34 oat accessions from the oat CORE panel at 3 and 7 days following germination (A and B, respectively). Measurement represents the angle between the outer most seminal roots. Error bars represent the 95% confidence interval of the mean. Comparison between the angles (C) reveals lack of correlation.

root traits are critical for oat lodging resistance. It also moves us forward in terms of developing methods for screening for oat lodging resistance. As we complete the screening of the diversity collection, we will identify new sources of root variation. As we complete the root phenotyping for the set of 22 oat genotypes across oat development (Section 9.1), we will develop a comprehensive understanding of root architectural changes that may contribute to lodging resistance.

9.3 Field Study Assessing Traits which may Impact Lodging (Oat1)

To begin to identify which traits are most critical for oat lodging in western Canada, field trials were accomplished in 2022 which assessed stem and root traits as well as panicle architecture.

Analysis of variance was conducted to understand the influence of genotype, location and their interaction on the field traits collected across the three locations in 2022. Significant genotypic variation was observed for all traits except stem force (and the related traits force per plant and force per panicle) and root volume. Location had a significant effect on all traits. Significant interaction between genotype and location was observed for height, stem strength, stem failure, root plate spread, root plate angle and outer stem diameter.

Table 1. Summary of linear mixed model effects determined for genotype, location and interaction on 22 traits across three field locations. Signficance, p<0.05*, 0.01**, 0.001***

Trait	Factor	Significance	Trait	Factor	Significance
Height	Genotype	***	ForcePerPanicle	Genotype	
	Location	***		Location	***
	Interaction	*		Interaction	
Flag_Angle	Genotype	***	RootPlateSpread	Genotype	***
	Location	***		Location	***
	Interaction			Interaction	*
Flag_1_Angle	Genotype	***	RootPlateDepth	Genotype	
	Location	***		Location	***
	Interaction			Interaction	
Flag_2_Angle	Genotype	*	RootPlateAngle	Genotype	***
	Location	*		Location	***
	Interaction			Interaction	*
NumPlants	Genotype	*	MinThick	Genotype	***
	Location	**		Location	***
	Interaction			Interaction	
NumPanicles	Genotype	***	OuterDiameter	Genotype	***
	Location	***		Location	***
	Interaction			Interaction	*
Internode2 Length	Genotype	***	InnerDiameter	Genotype	***
	Location	***		Location	***
	Interaction			Interaction	
StemStrength	Genotype	***	FieldSolidity	Genotype	***
	Location	***		Location	***
	Interaction	***		Interaction	
StemFailure	Genotype	***	Volume	Genotype	
	Location	***		Location	***
	Interaction	***		Interaction	
Force	Genotype		RootLength	Genotype	*
	Location	***		Location	**
	Interaction			Interaction	
ForcePerPlant	Genotype		SurfaceArea	Genotype	*
	Location	***		Location	***
	Interaction			Interaction	

Heritability values were calculated for all traits and are reported in Table 3. The most heritable field-measured traits were height (0.81), internode length (0.81) and flag leaf angle (0.80), the most heritable stem traits were outer diameter (0.84) and inner diameter (0.82), while the most heritable root trait was root plate spread (0.75). Due to their high heritability these traits would be useful to breeders if they demonstrate correlation to lodging resistance. A few traits are missing heritability values, and this could be due to lack of genetic variance at this stage.

Table 2. Heritability values calculated for 22 traits measured across three locations. RootPlateDepth and MaxWidth displayed zero genotypic variance and were not included.

Trait	Heritability
Height	0.81
Flag_Angle	0.80
Flag_1_Angle	0.77
Flag_2_Angle	0.48
NumPlants	0.47
NumPanicles	0.69
Internode2Length	0.81
StemStrength	0.36
StemFailure	0.49
Force	0.00
ForcePerPlant	0.13
ForcePerPlant	0.30
RootPlateSpread	0.75
RootPlateAngle	0.59
MinThick	0.75
OuterDiameter	0.84
InnerDiameter	0.82
FieldSolidity (Root Image)	0.57
Volume (Root Image)	0.38
RootLength (Root Image)	0.39
Depth (Root Image)	0.64
SurfaceArea (Root Image)	0.47

There was very minimal lodging in the 2022 trials, so all traits were compared to the assigned lodging ratings with very good (=2), good (=4), fair (=6), and poor (=8).

Relationships among the field data collected across the three locations were summarized into a correlation heatmap (Fig. 10). Lodging rating showed a significant positive relationship to height, flag leaf angle and internode length (r=0.40, 0.38 and 0.61, respectively), and a negative correlation with inner stem radius (r=-0.34). While many of these correlations are not overly strong, it will be interesting to observe how these relationships change with additional data that will be collected in 2023 trials.

There were also several correlations between stem and plant-related traits that are known to be connected to lodging resistance. For example, whole plant bending strength (or stem pushing resistance) when represented by force per head, was positively correlated to both outer and inner stem diameter (r=0.47 and 0.49, respectively), while the stem strength was positively correlated to minimum stem thickness and outer stem diameter (r=0.39 and 0.52, respectively). It was also interesting to note that the force for stem failure (stem strength) was positively correlated to height (r=0.36), but height was not correlated to stem diameter or minimum thickness traits.

The root imaging traits showed several interesting correlations with above-ground traits. For example, there was a positive correlation between height and root depth (r=0.33) and a negative correlation between flag leaf angle and root plate angle (r=-0.34). Amongst the root traits, not surprisingly solidity of the root system was influenced by both root volume (r=0.55) and root depth (r=-0.55). As described in section 9.1, solidity is defined as the ratio of the network area to convex area, with the convex area being the minimal sized convex polygon that can contain the root system (i.e. network area).

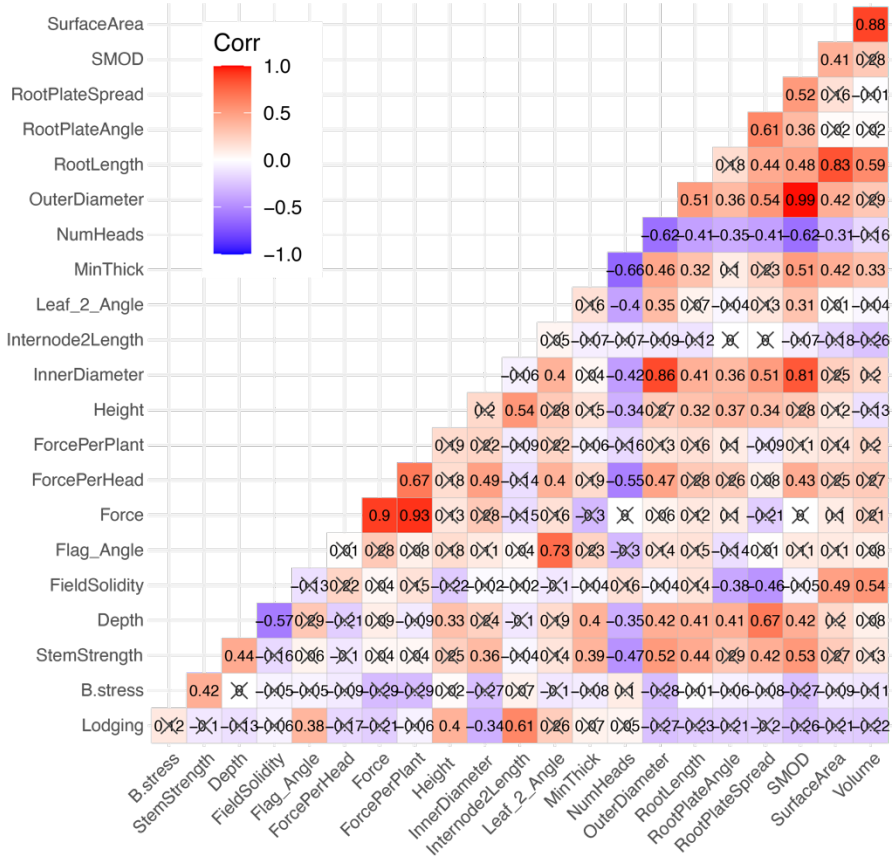

Fig. 10. Pearson correlation heat map among field collected data. All data was based on three site years except lodging which was based on values assigned to lodging categories. Relationships that were not significant (p<0.05) are crossed out.

Since inner stem diameter was correlated with lodging rating, we further investigated the variation in stem structure across the 14 oat genotypes (Fig. 11). Visual differences in both outer stem diameter and inner stem diameter of internode 2 were observed, creating variation in both overall stem size but also stem thickness (Fig. 11a). To further quantitate and visualize differences in stem strength and structure, we compared the stem bending stress to section modulus. Section modulus is a geometric property of a cross-section which represents the amount of material present and indicates stem thickness (Ookawa et al. 2016). The force required to induce stem failure (bending strength or bending moment) is related to section modulus; together the ratio of bending strength to section modulus represents the bending stress of a material. Comparing oat genotypes, AC Morgan and OT3071 consistently had large stems across field environments while others such as OT3112 and OT6007 had smaller thinner stems. Stem strength and related characteristics are critical for resistance to stem-based lodging (Mohammadi et al. 2020). Recently, wind tunnel experiments determined that oat can suffer from greater stem injury during bending motion than wheat (Gangwar et al. 2023). Stem strength and stem diameter are traits we will continue to investigate as the project proceeds.

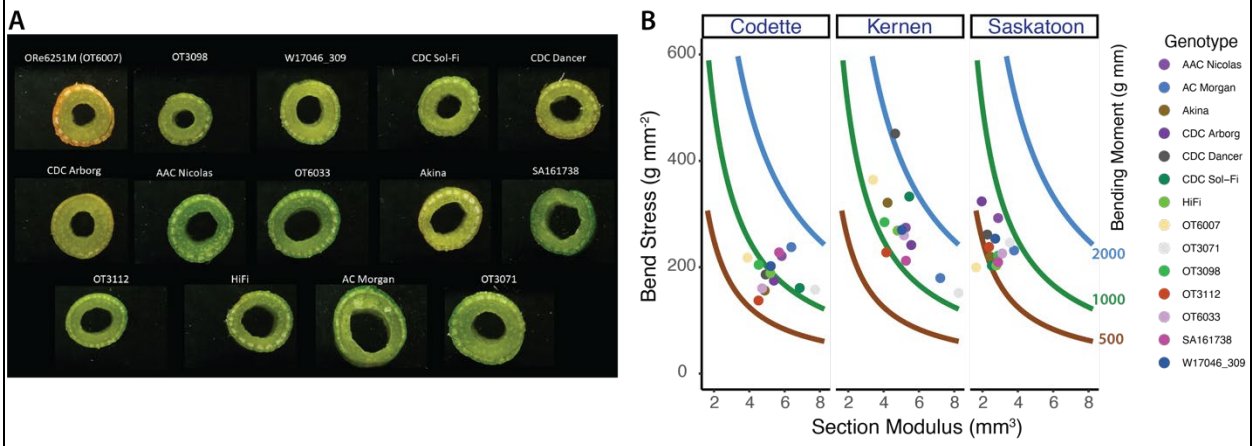

Fig. 11. Analyses of stems from 14 oat genotypes grown in replicated field trials at 3 locations. (A) Variation observed in stem outer and inner diameter. (B) Relationship between section modulus and bending stress. Curved lines the bending moment of the second internode.

Panicles were collected from 2 field sites in 2022, Codette and Kernen. The 14 oat genotypes displayed differences in panicle architecture (Fig. 12). CDC Sol-Fi and OT3071 had the largest panicle areas, both in terms of actual panicle pixels (network area) and also the space which they occupied (convex area). OT6007 and OT3098 had the smallest panicles but Akina also occupied a small convex area. In this respect, OT6007 and Akina had the narrowest panicle widths while Sol-Fi and OT3071 had the widest panicles. As the project moves forward, we will test 3D point cloud reconstructions of panicles and also begin to test the association of panicle traits to lodging.

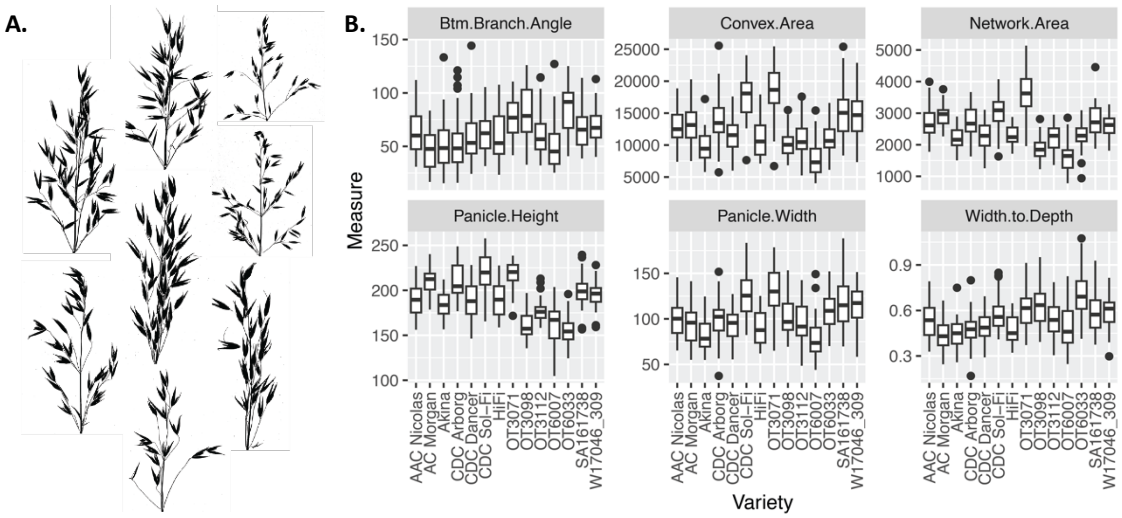

Fig. 12. Preliminary analysis of panicle architecture from 14 oat genotypes grown in replicated field trials at Codette and Kernen locations. (A) Select panicles segmented from background for analysis. (B) Distribution of data for six (6) panicle architectural traits. Btm.Branch.Angle represents the lower most panicle branch angle. Width.to.Depth represents the ratio of maximum width to depth.

9.4 Effect of Seeding Rate on Lodging-Related Traits (Oat2)

Analysis of variance was conducted to understand the influence of genotype, location, seeding rate and interaction between genotype and both location and seeding rate on the field traits collected across the two locations in 2022. Significant genotypic variation for height, number of panicles, internode length, stem strength and minimum stem thickness was observed while location was a significant effect for height, internode length, outer stem diameter and inner stem diameter (Table 3). Seeding rate influenced height, number of panicles, stem strength, minimum stem thickness, outer stem diameter and inner stem diameter (Table 3). No significant interactions were observed, and they were excluded from this table.

Relationships among the field data collected across the two locations were summarized into a correlation heatmap (Fig. 13). Seeding rate showed a significant positive correlation to number of plants (r=0.25) and a negative correlation with stem strength, stem failure, minimum stem thickness, and outer diameter (r=-0.32, -0.25, -0.24, -0.25, respectively).

There were also several correlations observed again between stem and plant-related traits, such as the stem strength-related traits (StemStrength and StemFailure) were positively correlated to minimum stem thickness, outer diameter, and inner diameter (r=0.43 to 0.77). It was also interesting to note that root plate spread was negatively correlated to number of plants and number of panicles (r=-0.29 and -0.5, respectively), but root plate spread was not correlated to seeding rate.

Table 3: Summary of linear mixed model effects determined for genotype, location and seeding rate on 13 traits measured across two field locations. Signficance levels, p<0.05*, 0.01**, 0.001***

Trait	Factor	Significance	Trait	Factor	Significance
Height	Genotype	***	RootPlateDepth	Genotype	
	Location	***		Location	
	SeedingRate	**		SeedingRate	
NumPlants	Genotype		RootPlateAngle	Genotype	
	Location			Location	
	SeedingRate	*		SeedingRate	
NumPanicles	Genotype	*	FieldSolidity	Genotype	
	Location			Location	
	SeedingRate	***		SeedingRate	
Internode2 Length	Genotype	***	MinThick	Genotype	*
	Location	***		Location	
	SeedingRate			SeedingRate	**
StemStrength	Genotype	**	OuterDiameter	Genotype	
	Location			Location	***
	SeedingRate	***		SeedingRate	***
Force	Genotype		InnerDiameter	Genotype	
	Location			Location	**
	SeedingRate			SeedingRate	**
RootPlateSpread	Genotype	*			
	Location				
	SeedingRate				

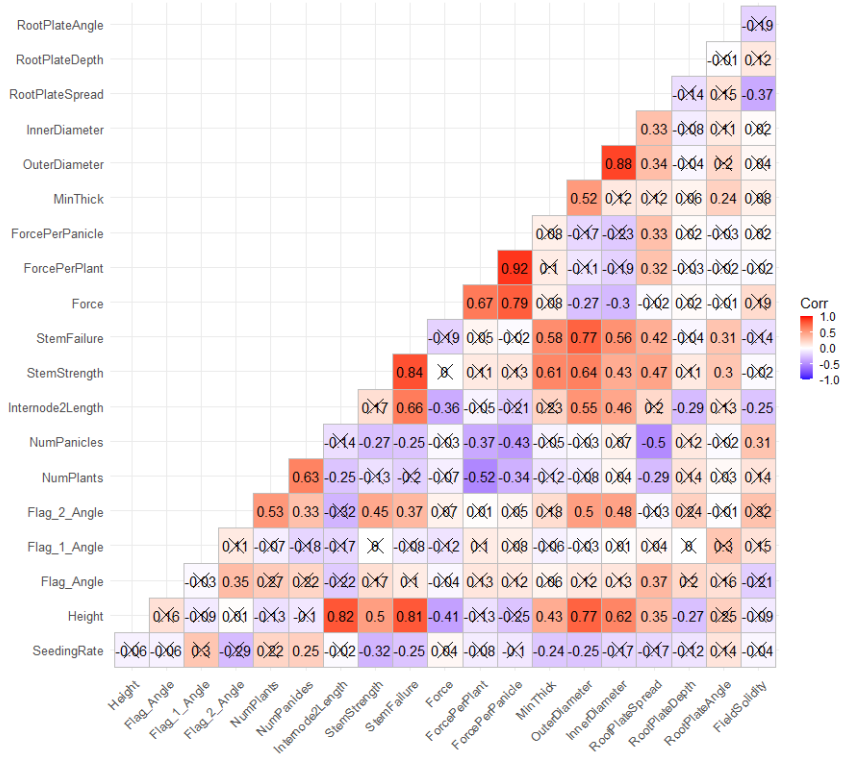

Fig. 13. Pearson correlation heat map among field collected data. All data was based on three site years except lodging which was based on values assigned to lodging categories. Relationships that are not significant ($p<0.05$) are crossed out.

Box plots were used to visualize the relationship between seeding rate and traits. All varieties showed similar response to seeding rates (data not shown). As an example, the impact of seeding rate on stem strength is shown in Figure 14. The increase in stem strength as seeding rate decreased was expected.

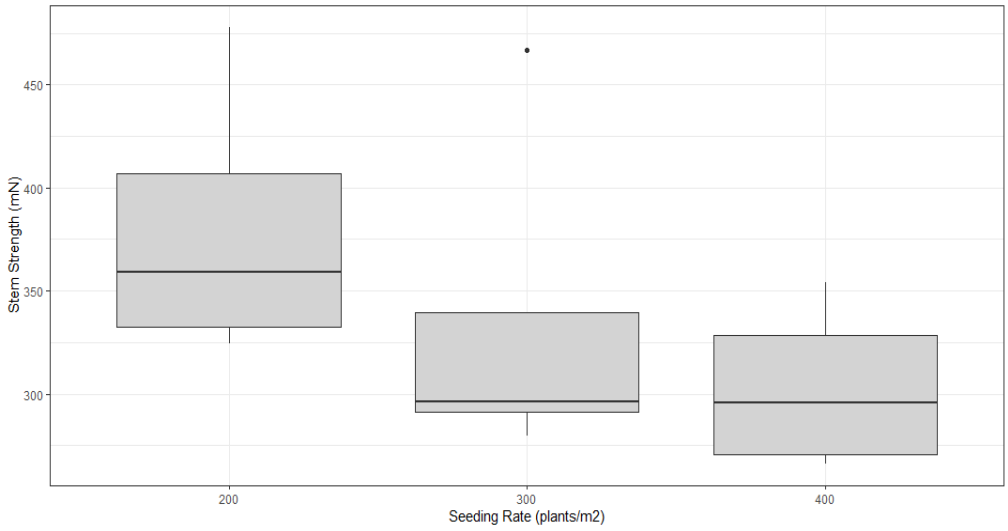

Fig. 14. Box plot demonstrating the relationship between seeding rate and stem strength amongst four oat genotypes grown at two locations in 2022.

10. Interim conclusions:

(*Maximum of 500 words)*.

Through the first 14 months of the project we have found significant associations of stem and root traits to field lodging rating. Above ground, there was a significant correlation to plant height with the highest positive correlation to lodging being length of the second internode. That height is correlated to lodging is not surprising. Taller plants create greater leverage forces, driven by wind, on both the root system but also on the stem itself. Height's impact on lodging is well documented in the cereal literature and we know that reductions in height helped to drive the green revolution in wheat and rice. The negative correlation of inner stem diameter to lodging rating suggests that stem strength may play a role; although stem thickness or other strength traits were not associated with lodging. The positive association of flag leaf angle with lodging rating is also potentially consistent with work by Wu and Ma (2019) who showed that more erect-leaf types have greater lodging resistance (in a study of 4 cultivars). Although we did not observe a relationship between field root traits and lodging resistance, it was reassuring that expected relationships such as the positive correlation between root angle and root plate spread were observed. Overall, following the first year of data collection and analysis, the project has made good progress in characterizing factors related to lodging resistance in oat. Pending weather outcomes in 2023, we hope to collect robust lodging data in year two of the field trials. This will enable a more thorough analysis of trait relationships to lodging resistance, not only for the field work but also for the indoor root phenotyping. Once sufficient data has been collected, it will be important to critically model the interactions between height, stem, root, and panicle traits in oat lodging resistance.

For root phenotyping, we have established that seminal root development is more complex in oat than other cereals such as barley and wheat. The angles of seminal roots emerging after germination are not correlated with those that emerge at germination. As the project continues to establish the framework for oat root system development from germination to maturity, we will be able to create robust phenotyping methods to capture root system angles representative of the genetics driving root plate spread. Phenotyping of mature root systems in rhizoboxes has demonstrated that we can capture the relationships between root system angle (spread) and lodging resistance. For example, the wider root angle of CDC Arborg suggests why it has very good lodging resistance even though it is a taller cultivar. That median root number was associated to lodging rating is interesting and will be followed up on. Finally, the screening of further diverse oat accessions will continue to reveal the root trait variation present. This is important for not only ensuring the best lodging resistant root traits are utilized for breeding, but also builds knowledge for future studies related to nutrient uptake or abiotic (drought/salt) stress tolerance.

11. List any technology transfer activities undertaken in relation to this project:

Include conference presentations, talks, papers published etc.

1. Ferré C, Beattie A, Feurtado JA. Understanding Lodging in Oat through Root, Stem, and Leaf Characteristics. Oral Presentation. 38th Annual Plant Graduate Students' Symposium between the University of Saskatchewan, University of Manitoba, and North Dakota State University. March 7-8, 2023.

12. Identify any changes expected to industry contributions, in-kind support, collaborations or other resources.

No changes identified to date after 14 months of project work. Of note, Céline Ferré, M.Sc. student on the project, was a Knowles Scholarship Recipient in 2022; valued at $25,000/year plus tuition for 2.5 years with $5,000 travel allowance.

13. Appendices: *Include any additional materials supporting the previous sections, e.g. detailed data tables, maps, graphs, specifications, literature cited (using a consistent reference style), acknowledgments*

Appendix 1, Additional Tables and Figures:

Table 1. Expanded set of oat genotypes used for field lodging trials and indoor controlled environment root phenotyping experiments. Genotypes highlighted in grey were used in the Oat1 lodging-trait field trial. Those marked with asterisk were used in the Oat2 seeding-rate trial.

ID	Genotype	Lodging Rating	Height (as % CS Camden)	Background	Type
1	CS Camden	Very Good	100 (=94 cm)	Sweden	Milling
2	OT3112*	Very Good	91	Canada (semi-dwarf)	Milling
3	OT3098	Very Good	91	Canada (semi-dwarf)	Milling
4	OT3071	Very Good	107	Canada	Milling
5	AC Morgan	Very Good	107	Canada	Milling
6	CDC Arborg*	Very Good	115	Canada/Sweden	Milling
7	AAC Nicolas	Good	107	Canada	Milling
8	Akina	Good	102	Sweden	Milling
9	CDC Ruffian	Fair	101	Canada	Milling
10	CDC Dancer	Fair	109	Canada	Milling
11	CDC Norseman	Fair	108	Canada	Milling
12	CDC Haymaker	Fair	120	Canada	Forage
13	OT6007*	Poor	102	Canada/US/Sweden	Milling
14	CDC SolFi*	Poor	116	Canada/US	Milling
17	HiFi	Poor	115	US	Milling
18	Newburg	Poor	115	US	Milling
19	CFA1809	Poor	115	Sweden	Milling
20	W17046_309	Poor	109	US	Milling
21	SA161738	Poor	125	Canada	Forage
22	SA161940	Poor	111	Canada/US	Forage
23	OT6033	Poor	90	Canada	Milling
24	HOT602	Poor	120	Canada	Hulless

Table 2. Oat CORE Diversity Panel.

ID	Origin	Entry	Name
CORE001	CORE SSK	001	Sun II-1
CORE002	CORE SSK	002	Hurdal
CORE003	CORE SSK	003	Morgan_AC
CORE004	CORE SSK	004	Marion (Canada)
CORE005	CORE SSK	005	Goslin
CORE006	CORE SSK	006	Asencao
CORE007	CORE SSK	007	Ajay
CORE008	CORE SSK	008	Ogle
CORE009	CORE SSK	009	Rigodon_AC
CORE010	CORE SSK	010	Gem
CORE011	CORE SSK	011	Morton
CORE012	CORE SSK	012	Marie_AC
CORE013	CORE SSK	013	Dancer_CDC
CORE014	CORE SSK	014	Assiniboia/S42
CORE015	CORE SSK	015	Buckskin
CORE016	CORE SSK	016	HiFi
CORE017	CORE SSK	017	TAM O-301
CORE018	CORE SSK	018	Coker 227
CORE019	CORE SSK	019	Kanota

CORE020	CORE SSK	020	Kangaroo
CORE021	CORE SSK	021	CI 4706-2
CORE022	CORE SSK	022	Tardis
CORE023	CORE SSK	023	Buffalo
CORE024	CORE SSK	024	Maverick
CORE025	CORE SSK	025	Calibre
CORE026	CORE SSK	026	Dane
CORE027	CORE SSK	027	Florida 501
CORE028	CORE SSK	028	Jay
CORE029	CORE SSK	029	Jerry
CORE030	CORE SSK	030	Ronald_AC
CORE031	CORE SSK	031	Sesqui
CORE032	CORE SSK	032	Sol-Fi_CDC
CORE033	CORE SSK	033	TAM O-397
CORE034	CORE SSK	034	Triple Crown
CORE035	CORE SSK	035	Troy
CORE036	CORE SSK	036	Aarre
CORE037	CORE SSK	037	Baler_CDC
CORE038	CORE SSK	038	Blaze
CORE039	CORE SSK	039	Boyer_CDC
CORE040	CORE SSK	040	Drummond
CORE041	CORE SSK	041	Furlong
CORE042	CORE SSK	042	IL86-5698-3
CORE043	CORE SSK	043	Kaufman
CORE044	CORE SSK	044	MAM 17-5
CORE045	CORE SSK	045	OT380
CORE046	CORE SSK	046	ProFi_CDC
CORE047	CORE SSK	047	SO-1
CORE048	CORE SSK	048	Vista
CORE049	CORE SSK	049	MN841801-1
CORE050	CORE SSK	050	Mortlock
CORE051	CORE SSK	051	Noble-2
CORE052	CORE SSK	052	Maldwyn
CORE053	CORE SSK	053	Gehl
CORE054	CORE SSK	054	Coker 234
CORE055	CORE SSK	055	WAOAT2132
CORE056	CORE SSK	056	OA1063-8
CORE057	CORE SSK	057	Prescott
CORE058	CORE SSK	058	Robust
CORE059	CORE SSK	059	Shadow
CORE060	CORE SSK	060	Belinda
CORE061	CORE SSK	061	Dominik (Bauer)
CORE062	CORE SSK	062	Matilda
CORE063	CORE SSK	063	Sang
CORE064	CORE SSK	064	SW Betania
CORE065	CORE SSK	065	Pg11
CORE066	CORE SSK	066	Pg16
CORE067	CORE SSK	067	Ajax
CORE068	CORE SSK	068	Cherokee
CORE069	CORE SSK	069	Z615-4
CORE070	CORE SSK	070	Boudrias
CORE071	CORE SSK	071	UFRGS 8
CORE072	CORE SSK	072	UFRGS 881971
CORE073	CORE SSK	073	UFRGS 930605
CORE074	CORE SSK	074	Centennial
CORE075	CORE SSK	075	Dal
CORE076	CORE SSK	076	Exeter
CORE077	CORE SSK	077	OT586

CORE078	CORE SSK	078	Pinnacle_AC
CORE079	CORE SSK	079	MF9522-523
CORE080	CORE SSK	080	Freddy
CORE081	CORE SSK	081	Melys
CORE082	CORE SSK	082	Ranch
CORE083	CORE SSK	083	Bountiful
CORE084	CORE SSK	084	CIav 6209
CORE085	CORE SSK	085	Ford Early Giant
CORE086	CORE SSK	086	Novojatkovo
CORE087	CORE SSK	087	Pusa Hybrid G
CORE088	CORE SSK	088	Akiyutaka
CORE089	CORE SSK	089	Provena
CORE090	CORE SSK	090	Chaps
CORE091	CORE SSK	091	Flaemingsnova
CORE092	CORE SSK	092	Fulghum
CORE093	CORE SSK	093	Lang
CORE094	CORE SSK	094	Lutz
CORE095	CORE SSK	095	Otana
CORE096	CORE SSK	096	Pacer_CDC
CORE097	CORE SSK	097	Salomon
CORE098	CORE SSK	098	Urano
CORE099	CORE SSK	099	Chernigovskij 27B
CORE100	CORE SSK	100	Clinton
CORE101	CORE SSK	101	H927-1-6-1-x-x-24
CORE102	CORE SSK	102	Hazel
CORE103	CORE SSK	103	MN 811045
CORE104	CORE SSK	104	Red Rustproof
CORE105	CORE SSK	105	Russell
CORE106	CORE SSK	106	Stout
CORE107	CORE SSK	107	Ukraine reselection
CORE108	CORE SSK	108	Victoria
CORE109	CORE SSK	109	Bia
CORE110	CORE SSK	110	Maverick
CORE111	CORE SSK	111	TAMO-406
CORE112	CORE SSK	112	Leggett
CORE113	CORE SSK	113	Rodgers
CORE114	CORE SSK	114	Horizon270

Table 3. Oat root trait descriptions for controlled environment experiments. Following description of the root trait, square brackets enclose the unit of measurement. Numbers within the trait abbreviation present the days after germination at which the trait was measured (e.g. SR.ang.3 = seminal root emergence angle at 3 days after germination).

Trait Abbreviation	Trait	Description	Experiment	Software
SR.ang.3	Seminal Root Emergence Angle	The angle between the outermost paths of seminal root growth (following emergence from the grain). [degree]	Seminal Root Emergence Angle	ImageJ
Median.roots (Med.Rt.17)	Median Number of Roots	The result of a vertical line sweep in which the number of roots that crossed a horizontal line was estimated, and then the median of all values for the extent of the network was calculated. [n]	2D Pouch Hydroponic	RhizoVision Explorer
Max.roots (Max.Rt.17)	Maximum Number of Roots	After sorting the number of roots crossing a horizontal line from smallest to largest, the maximum	2D Pouch Hydroponic	RhizoVision Explorer

		number is considered to be the 84th-percentile value (one standard deviation). [n]		
Root.tips (Tips.17)	Number of Root Tips	Number of root tips in the image. [n]	2D Pouch Hydroponic	RhizoVision Explorer
Root.length (Length.17)	Total Root Length	Cumulative length of all the roots. [mm]	2D Pouch Hydroponic	RhizoVision Explorer
Depth (Depth.17)	Depth	The length in the vertical direction from the upper-most network pixel to the lower-most network pixel. [mm]	2D Pouch Hydroponic	RhizoVision Explorer
Max.width (Width.17)	Maximum Width	The length in the horizontal direction from the left-most network pixel to the right-most network pixel. [mm]	2D Pouch Hydroponic	RhizoVision Explorer
Width.depth.ratio (WDR.17)	Width-to-Depth Ratio	The value of network width divided by the value of network depth. [mm/mm]	2D Pouch Hydroponic	RhizoVision Explorer
Network.area (Net.Area.17)	Network Area	The network area is the total number of pixels in the segmented image. [mm^2]	2D Pouch Hydroponic	RhizoVision Explorer
Convex.area (C.Area.17)	Convex Area	The area of the convex hull that encompasses the root. [mm^2]	2D Pouch Hydroponic	RhizoVision Explorer
Solidity (Solidity.17)	Solidity	The total network area divided by the network convex area. [mm^2/mm^2]	2D Pouch Hydroponic	RhizoVision Explorer
Lower.root.area (Low.Area.17)	Lower Root Area	The lower root area is the area of the segmented image pixels that are located below the location of the medial axis pixel that has the maximum radius. [mm^2]	2D Pouch Hydroponic	RhizoVision Explorer
Avg.diameter (Avg.Dia.17)	Average Diameter	The mean value of the root width estimation computed for all pixels of the medial axis of the entire root system. [mm]	2D Pouch Hydroponic	RhizoVision Explorer
Median.diameter (Med.Dia.17)	Median Diameter	The median value of the root width estimation computed for all pixels of the medial axis of the entire root system. [mm]	2D Pouch Hydroponic	RhizoVision Explorer
Max.diameter (Max.Dia.17)	Maximum Diameter	The maximum value of the root width estimation computed for all pixels of the medial axis of the entire root system. [mm]	2D Pouch Hydroponic	RhizoVision Explorer
Perimeter (Perim.17)	Perimeter	Perimeter is the count of the total number of pixels in the perimeter image. [mm]	2D Pouch Hydroponic	RhizoVision Explorer
Volume (Vol.17)	Volume	The sum of the local volume at each pixel of the network skeleton, as approximated by a tubular shape whose radius is estimated from the image. [mm^3]	2D Pouch Hydroponic	RhizoVision Explorer
Surface.Area (SA.17)	Surface Area	The sum of the surface area at each pixel of the network skeleton, as approximated by a tubular shape whose radius is estimated from the image. [mm^2]	2D Pouch Hydroponic	RhizoVision Explorer

Holes (Holes.17)	Holes	Holes are the disconnected background components and indicative of root branching and complexity. They can be counted by inverting the segmented image.	2D Pouch Hydroponic	RhizoVision Explorer
Avg.Hole (Hole.Size.17)	Average Hole Size	The average hole size (area) is calculated. [mm^2]	2D Pouch Hydroponic	RhizoVision Explorer
Avg.Orientation (Avg.Orient.17)	Average Root Orientation	For every medial axis pixel, the orientation at the pixel is computed by determining the mean orientation of medial axis pixels in a 40x40 pixel locality. The average of all these orientations is noted as average root orientation. [degree]	2D Pouch Hydroponic	RhizoVision Explorer
Shallow.Freq (Shal.Angle.17)	Shallow Angle Frequency	Given the skeletal image, for every pixel in the medial axis, we get the locations of the medial axis pixels in a 40x40 pixel locality and determine the orientation of these pixels in the locality. This orientation is noted for every medial axis pixel. Given these orientations, we calculate the frequency in bins less than 30 degree.	2D Pouch Hydroponic	RhizoVision Explorer
Med.Freq (Med.Ang.17)	Medium Angle Frequency	Given the skeletal image, for every pixel in the medial axis, we get the locations of the medial axis pixels in a 40x40 pixel locality and determine the orientation of these pixels in the locality. This orientation is noted for every medial axis pixel. Given these orientations, we calculate the frequency in bins less than 60 degree.	2D Pouch Hydroponic	RhizoVision Explorer
Steep.Freq (Steep.Ang.17)	Steep Angle Frequency	Given the skeletal image, for every pixel in the medial axis, we get the locations of the medial axis pixels in a 40x40 pixel locality and determine the orientation of these pixels in the locality. This orientation is noted for every medial axis pixel. Given these orientations, we calculate the frequency in bins less than 90 degree.	2D Pouch Hydroponic	RhizoVision Explorer

Table 4. Trait descriptions for stem and root traits assessed in the 2022 field trials.

Trait Abbreviation	Trait	Description	Experiment / Trait Set
LodgingRating	Lodging rating	Pre-determined lodging ratings given to varieties in Saskatchewan Seed Guide	Agronomic Evaluation
Height	Height	Height of plants from soil to highest point without extending any of the panicle (cm)	Agronomic Evaluation
Flag_Angle	Flag leaf angle	Angle between top flag leaf and stem (°)	Leaf Evaluation
Flag_1_Angle	Second leaf angle	Angle between second leaf and stem (°)	Leaf Evaluation
Flag_2_Angle	Third leaf angle	Angle between third leaf and stem (°)	Leaf Evaluation
NumPlants	Number of Plants	Number of plants in 1m section measured by Stalker	Stem Resistance Evaluation
NumPanicles	Number of Panicles	Number of panicles in 1m section measured by Stalker	Stem Resistance Evaluation
Force	Stalker value	Maximum force required to push over row; collected using Stalker	Stem Resistance Evaluation
ForcePerPlant	Force per plant	Found by dividing Force by NumPlants	Stem Resistance Evaluation
ForcePerPanicle	Force per panicle	Found by dividing Force by NumPanicles	Stem Resistance Evaluation
Internode2Length	Internode length	Length of second internode (first full internode above soil) that was used for 3-point bend test and stem cross section imaging (mm)	Field Stem Evaluation
StemStrength	Bend test value	Maximum force required to bend second internode in 3-point bend test (mN)	Field Stem Evaluation
StemFailure	Stem failure point	Found using equation 2 above.	Field Stem Evaluation
MinThick	Minimum stem wall thickness	Minimum stem wall thickness, as measured on stem cross section images (mm)	Field Stem Evaluation
OuterDiameter	Outer stem wall diameter	Diameter of outer stem wall, as measured on stem cross section images (mm)	Field Stem Evaluation
InnerDiameter	Inner stem wall diameter	Diameter of inner stem wall, as measured on stem cross section images (mm)	Field Stem Evaluation
RootPlateSpread	Root plate spread	Widest point of root system, manually measured on field root samples (cm)	Field root Evaluation
RootPlateDepth	Root plate depth	Structural depth of root system, manually measured on field root samples (cm)	Field root

			Evaluation
RootPlateAngle	Root plate angle	Widest angle of root system, manually measured on field root samples (°)	Field root Evaluation
FieldSolidity	Solidity	The total network area divided by the network convex area, the area of the convex hull that encompasses the root (cm^2/cm^2)	Field Root Image Analysis
Volume	Total root volume	The sum of the local volume at each pixel of the network skeleton, as approximated by a tubular shape whose radius is estimated from the image. (cm^3)	Field Root Image Analysis
RootLength	Total root system length	Total network length divided by network volume. (cm/cm^2)	Field Root Image Analysis
Depth	Root system depth	The length in the vertical directions from the upper-most network pixel to the lower-most network pixel. (cm)	Field Root Image Analysis
MaxWidth	Maximum root system width	The length in the horizontal direction from the left-most network pixel to the right-most network pixel. (cm)	Field Root Image Analysis
SurfaceArea	Root system surface area	The sum of the surface area at each pixel of the network skeleton, as approximately by a tubular shape whose radius is estimated form the image. (cm^2)	Field Root Image Analysis

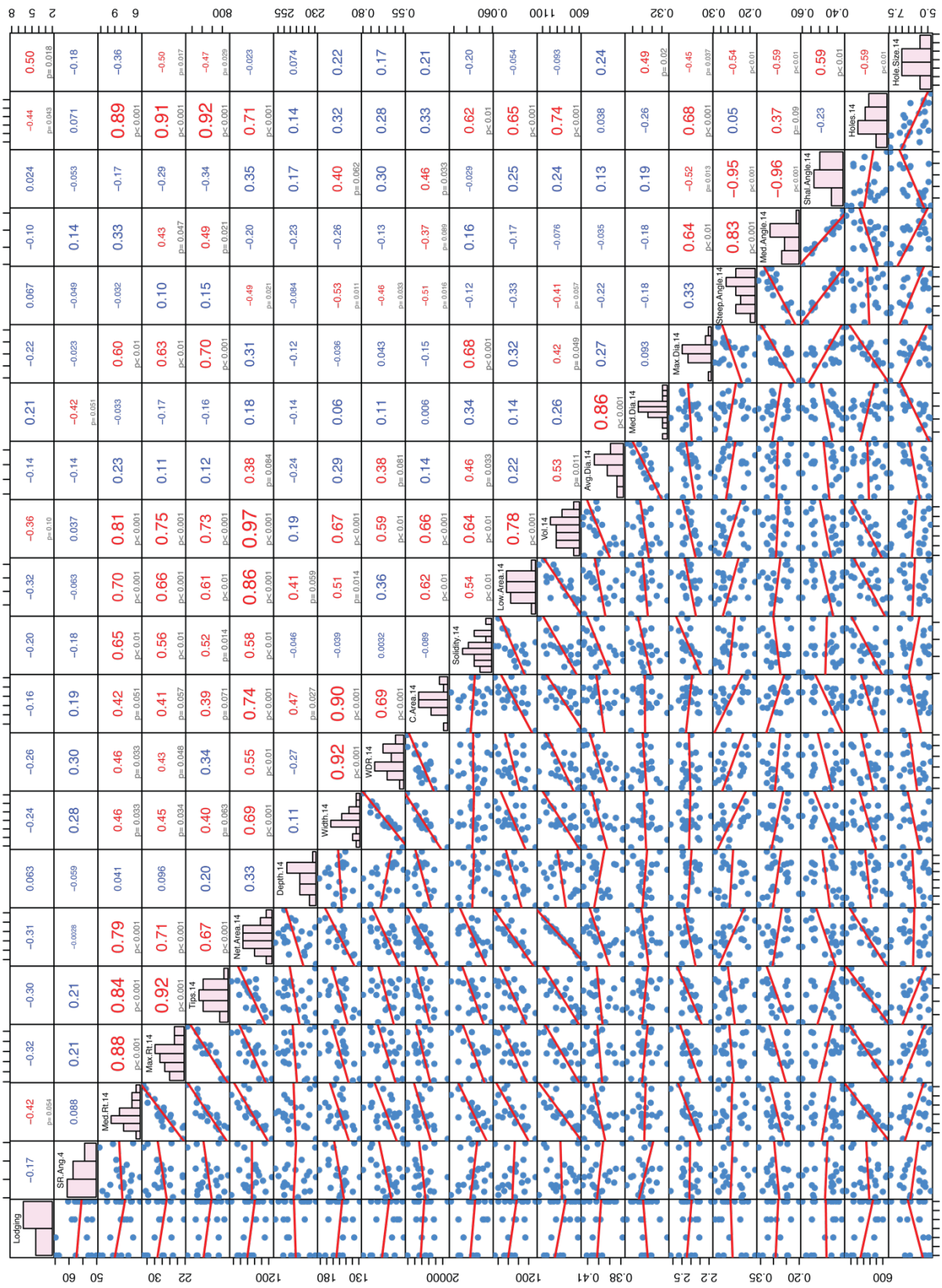

Fig. 1. Oat root system images captured 14 days following germination from 2D pouch hydroponics. Data represent seminal angle and 19 root traits compared to lodging rating of 22 oat genotypes in Appendix – Table 1. Upper panel represents Pearson correlation coefficents with red colours being significant.

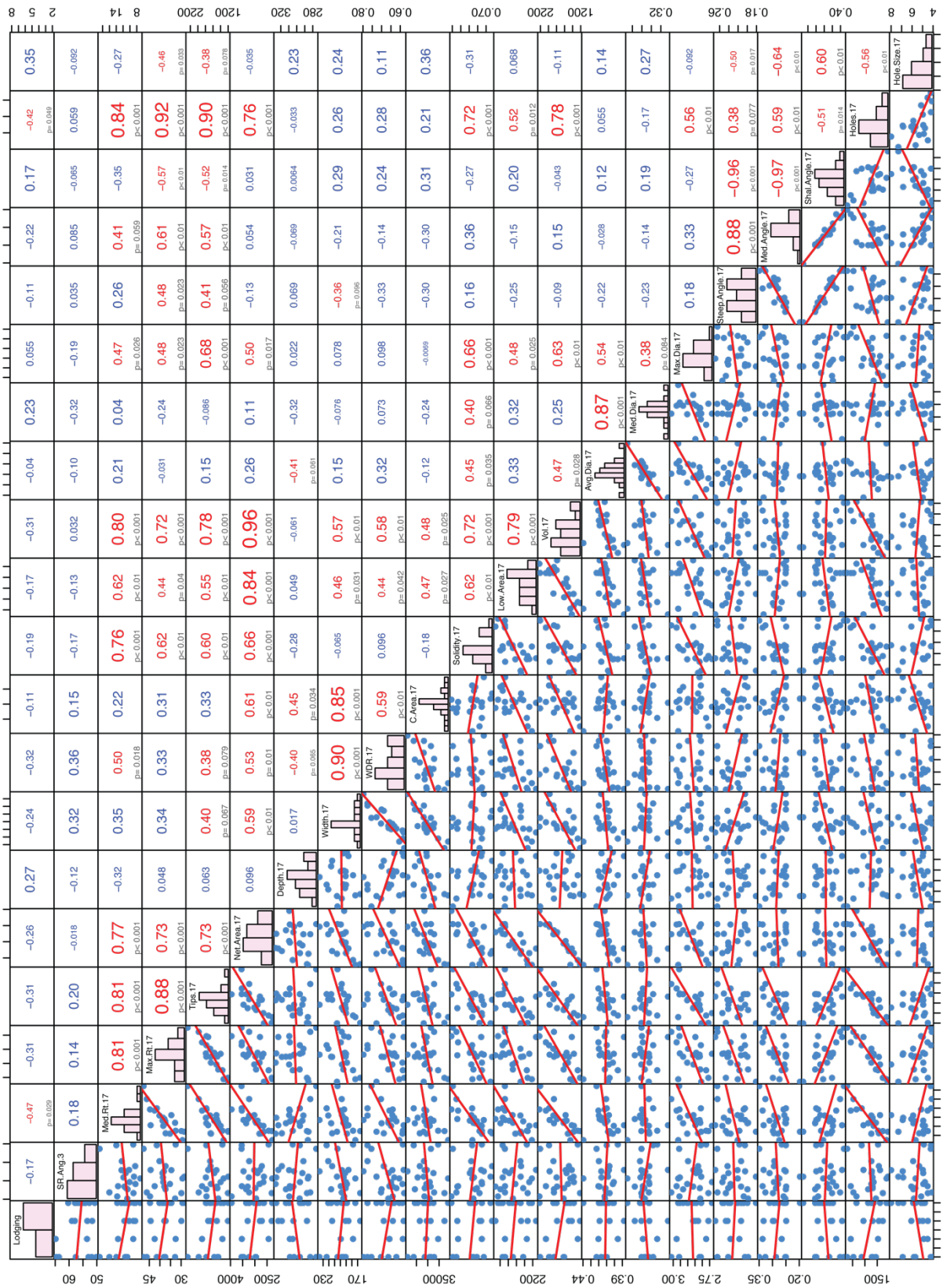

Fig. 2. Oat root system images captured 17 days following germination from 2D pouch hydroponics. Data represent seminal angle and 19 root traits compared to lodging rating of 22 oat genotypes in Appendix – Table 1. Upper panel represents Pearson correlation coefficents with red colours being significant.

Appendix 2, References:

Aidoo, J. P. (2017). Optimizing Oat Yield, Quality and Stand-ability in Central Alberta. Available at: https://era.library.ualberta.ca/items/290e8976-4ad2-4fdf-b1d0-3d0335c37c97 .

Baker, C. J., Sterling, M., and Berry, P. (2014). A generalised model of crop lodging. Journal of Theoretical Biology 363, 1–12. doi: 10.1016/j.jtbi.2014.07.032.

Berry, P. M., Sterling, M., Baker, C. J., Spink, J., and Sparkes, D. L. (2003). A calibrated model of wheat lodging compared with field measurements. Agricultural and Forest Meteorology 119, 167–180. doi: 10.1016/S0168-1923(03)00139-4.

Berry, P. M., Sterling, M., and Mooney, S. J. (2006). Development of a Model of Lodging for Barley. J Agron Crop Sci 192, 151–158. doi: 10.1111/j.1439-037X.2006.00194.x.

Berry, P. M., Sterling, M., Spink, J. H., Baker, C. J., Sylvester-Bradley, R., Mooney, S. J., et al. (2004). Understanding and Reducing Lodging in Cereals. Advances in Agronomy 84, 217–271. doi: 10.1016/S0065-2113(04)84005-7.

Bolker, B., and Robinson, D. (2021). broom.mixed: Tidying Methods for Mixed Models. Available at: https://CRAN.R-project.org/package=broom.mixed

Brinkman, M. A., and Rho, Y. D. (1984). Response of Three Oat Cultivars to N Fertilizer1. Crop Science 24, cropsci1984.0011183X002400050035x. doi: 10.2135/cropsci1984.0011183X002400050035x.

Buerstmayr, H., Krenn, N., Stephan, U., Grausgruber, H., and Zechner, E. (2007). Agronomic performance and quality of oat (Avena sativa L.) genotypes of worldwide origin produced under Central European growing conditions. Field Crops Research 101, 343–351. doi: 10.1016/j.fcr.2006.12.011.

Cullis, B. R., Smith, A. B., and Coombes, N. E. (2006). On the design of early generation variety trials with correlated data. JABES 11, 381–393. doi: 10.1198/108571106X154443.

de Rocquigny, P. J., Entz, M. H., Gentile, R. M., and Duguid, S. D. (2004). Yield Physiology of a Semidwarf and Tall Oat Cultivar. Crop Science 44, 2116–2122. doi: 10.2135/cropsci2004.2116.

Duy, P. Q., Abe, A., Hirano, M., Sagawa, S., and Kuroda, E. (2004). Analysis of Lodging-Resistant Characteristics of Different Rice Genotypes Grown under the Standard and Nitrogen-Free Basal Dressing Accompanied with Sparse Planting Density Practices. Plant Production Science 7, 243–251. doi: 10.1626/pps.7.243.

Ennos, A. R. (1991). The Mechanics of Anchorage in Wheat Triticum aestivum L.: II. ANCHORAGE OF MATURE WHEAT AGAINST LODGING. Journal of Experimental Botany 42, 1607–1613. doi: 10.1093/jxb/42.12.1607.

Gangwar, T., Susko, A. Q., Baranova, S., Guala, M., Smith, K. P., and Heuschele, D. J. (2023). Multi-scale modelling predicts plant stem bending behaviour in response to wind to inform lodging resistance. Royal Society Open Science 10, 221410. doi: 10.1098/rsos.221410.

Gardiner, B., Berry, P., and Moulia, B. (2016). Review: Wind impacts on plant growth, mechanics and damage. Plant Science 245, 94–118. doi: 10.1016/j.plantsci.2016.01.006.

Hedden, P. (2003). The genes of the Green Revolution. Trends in Genetics 19, 5–9. doi: 10.1016/S0168-9525(02)00009-4.

Kassambara, A. (2022). ggcorrplot: Visualization of a Correlation Matrix using “ggplot2”. Available at: https://CRAN.R-project.org/package=ggcorrplot.

Klos, K. E., Huang, Y.-F., Bekele, W. A., Obert, D. E., Babiker, E., Beattie, A. D., et al. (2016). Population Genomics Related to Adaptation in Elite Oat Germplasm. The Plant Genome 9, plantgenome2015.10.0103. doi: 10.3835/plantgenome2015.10.0103.

Kuchynková, H., and Pexová Kalinová, J. (2021). Influence of variety and growing conditions on Fusarium occurrence, mycotoxicological quality, and yield parameters of hulled oats. CEREAL RESEARCH COMMUNICATIONS 49, 577–585. doi: 10.1007/s42976-021-00133-5.

Kuznetsova, A., Brockhoff, P. B., and Christensen, R. H. B. (2017). lmerTest Package: Tests in Linear Mixed Effects Models. Journal of Statistical Software 82, 1–26. doi: 10.18637/jss.v082.i13.

Langseth, W., and Stabbetorp, H. (1996). The Effect of Lodging and Time of Harvest on Deoxynivalenol Contamination in Barley and Oats. Journal of Phytopathology 144, 241–245. doi: 10.1111/j.1439-0434.1996.tb01523.x.

Li, P., Mo, F., Li, D., Ma, B.-L., Yan, W., and Xiong, Y. (2018). Exploring agronomic strategies to improve oat productivity and control weeds: leaf type, row spacing, and planting density. Can. J. Plant Sci. 98, 1084–1093. doi: 10.1139/cjps-2017-0354.

Magnavaca, R., Gardner, C. O., and Clark, R. B. (1987). "Evaluation of inbred maize lines for aluminum tolerance in nutrient solution," in Genetic Aspects of Plant Mineral Nutrition, eds. W. H. Gabelman and B. C. Loughman (Dordrecht: Springer Netherlands), 255–265. doi: 10.1007/978-94-009-3581-5_23.

Marshall, H. G., Kolb, F. L., and Roth, G. W. (1987). Effects of Nitrogen Fertilizer Rate, Seeding Rate, and Row Spacing on Semidwarf and Conventional Height Spring Oat1. Crop Science 27, cropsci1987.0011183X002700030031x. doi: 10.2135/cropsci1987.0011183X002700030031x.

May, W. E., Brandt, S., and Hutt-Taylor, K. (2020). Response of oat grain yield and quality to nitrogen fertilizer and fungicides. Agronomy Journal 112, 1021–1034. doi: 10.1002/agj2.20081.

May, W. E., Mohr, R. M., Lafond, G. P., Johnston, A. M., and Craig Stevenson, F. (2004). Effect of nitrogen, seeding date and cultivar on oat quality and yield in the eastern Canadian prairies. Can. J. Plant Sci. 84, 1025–1036. doi: 10.4141/P04-044.

Milach, S. C. K., Rines, H. W., Phillips, R. L., Stuthman, D. D., and Morikawa, T. (1998). Inheritance of a New Dwarfing Gene in Oat. Crop Science 38, cropsci1998.0011183X003800020013x. doi: 10.2135/cropsci1998.0011183X003800020013x.

Mohammadi, M., Finnan, J., Sterling, M., and Baker, C. (2020). A calibrated oat lodging model compared with agronomic measurements. Field Crops Research 255, 107784. doi: 10.1016/j.fcr.2020.107784.

Molnar, S. J., Chapados, J. T., Satheeskumar, S., Wight, C. P., Bancroft, B., Orr, W., et al. (2012). Comparative mapping of the oat Dw6/dw6 dwarfing locus using NILs and association with vacuolar proton ATPase subunit H. Theor Appl Genet 124, 1115–1125. doi: 10.1007/s00122-011-1773-7.

Ookawa, T., Aoba, R., Yamamoto, T., Ueda, T., Takai, T., Fukuoka, S., et al. (2016). Precise estimation of genomic regions controlling lodging resistance using a set of reciprocal chromosome segment substitution lines in rice. Sci Rep 6, 30572. doi: 10.1038/srep30572.

Peterson, B. G., and Carl, P. (2020). PerformanceAnalytics: Econometric Tools for Performance and Risk Analysis. Available at: https://CRAN.R-project.org/package=PerformanceAnalytics .

R Core Team (2021). R: A language and environment for statistical computing. Available at: https://www.R-project.org/ .

Reynolds, M., Foulkes, M. J., Slafer, G. A., Berry, P., Parry, M. A. J., Snape, J. W., et al. (2009). Raising yield potential in wheat. Journal of Experimental Botany 60, 1899–1918. doi: 10.1093/jxb/erp016.

RStudio Team (2021). RStudio: Integrated Development for R. Available at: https://www.rstudio.com/ .

Schneider, C. A., Rasband, W. S., and Eliceiri, K. W. (2012). NIH Image to ImageJ: 25 years of image analysis. Nat Methods 9, 671–675. doi: 10.1038/nmeth.2089.

Sechler, D. T. (1961). Root Development and Lodging Resistance in Oats. Missouri Agricultural Experiment Station Research Bulletin. Available at: https://mospace.umsystem.edu/xmlui/handle/10355/58010 .

Seethepalli, A., Dhakal, K., Griffiths, M., Guo, H., Freschet, G. T., and York, L. M. (2021). RhizoVision Explorer: open-source software for root image analysis and measurement standardization. AoB PLANTS 13, plab056. doi: 10.1093/aobpla/plab056.

Shah, A. N., Tanveer, M., Rehman, A. ur, Anjum, S. A., Iqbal, J., and Ahmad, R. (2017). Lodging stress in cereal—effects and management: an overview. Environ Sci Pollut Res 24, 5222–5237. doi: 10.1007/s11356-016-8237-1.

Tumino, G., Voorrips, R. E., Morcia, C., Ghizzoni, R., Germeier, C. U., Paulo, M.-J., et al. (2017). Genome-wide association analysis for lodging tolerance and plant height in a diverse European hexaploid oat collection. Euphytica 213, 163. doi: 10.1007/s10681-017-1939-8.

Wickham, H., Averick, M., Bryan, J., Chang, W., McGowan, L. D., François, R., et al. (2019). Welcome to the Tidyverse. Journal of Open Source Software 4, 1686. doi: 10.21105/joss.01686.

Wright, K. (2021). pals: Color Palettes, Colormaps, and Tools to Evaluate Them. Available at: https://CRAN.R-project.org/package=pals .

Wu, W., and Ma, B.-L. (2019). Erect–leaf posture promotes lodging resistance in oat plants under high plant population. European Journal of Agronomy 103, 175–187. doi: 10.1016/j.eja.2018.12.010.

Zadoks, J. C., Chang, T. T., and Konzak, C. F. (1974). A decimal code for the growth stages of cereals. Weed Res 14, 415–421. doi: 10.1111/j.1365-3180.1974.tb01084.x.